An Investigation on Thermal Impacts on Space Vehicle Hydro Control System

By

Most Nusrat Gazi, M.Eng. (Electronics)

Supervisors: Prof. Dr. Fangpo He &

Dr. Amir Zanj

Date of Submission: October 2018

Submitted to the College of Science and Engineering, and Mathematics in the College of Science and Engineering in partial completion of the requirements for the degree of Master of Engineering (electronics) at Flinders university-Adelaide South Australia

Declaration

I certify that this work does not incorporate without acknowledgement any material previously submitted for a degree or diploma in any university, and that to the best of my knowledge and belief it does not contain any material previously published or written by another person except where due reference is made in the text.

Most Nusrat Gazi

October,2018

Acknowledgement

First, I would like to thank my supervisors, prof. Fangpo He and Amir Zanj for their encouragements and immense support to my project. I really appreciate all those technical supports and valuable time that they have given for my project. They have always inspired me to be consistent and confident with my project work.

And I am also thankful to all related staff, my friends for their patience and valuable advice during my project.

Finally, I would like to thank my mother for allowing me to go for post-graduation. I would never be able to come here (Australia) without her unconditional supports and inspirations.

Abstract

Investigating the dynamics of any multi-physical non-linear system has always received an extra attention in research sector. It becomes more challenging when investigation is performed on such multi-physical system under thermal condition. This thesis will reflect the importance of the investigation for modelling multi-physical interactive structural-dilation and property- changing behaviours of the system under severe thermal conditions. Through this project, the dynamic behaviour of the proposed pressure control valve is investigated under thermal conditions by means of Bond-graph technique. At first, a significant modification of the existing pressure control valve is done where the adjusting part of the valve is simplified in order to avoid the complexities related to interaction with moving elements and to achieve a much simple Bond-graph representation of the valve. Initially this pressure control valve had three moving elements (as shown in Fig.16). They are: control spool (spindle), adjusting spool and adjusting plate or placoid. The simplification is performed based on the scenario where the displacement of the adjusting spool and plate were happening concurrently. The resultant simplified Bond-graph model of the pressure control valve is more effective than the existing one with less number of state variables to be used to carry out the thermal investigation. Then a nonlinear mathematical model of that specific SLV (space launch vehicle) pressure control valve is built with respect to the simplified Bond-graph model. At this stage, different operating conditions that involve various inlet pressures is dynamically simulated. The obtained results are similar as the original ones which indicates that the pressure control regulator is working as per expectation with its simplified version. After this simplification, the Bond-graph models of both the elastic control and adjusting spool is developed. Then, the existing rigid adjusting spool of the control valve is replaced with the elastic one as the thermal conditions cannot be investigated with the rigid spool configuration. The characteristics of dilation and shrinking of the elastic spool can reveal the thermal impact precisely. Then the mathematical model of the control valve with elastic adjusting spool has been derived from the respective Bond-graph model and the obtained results reveal that the control valve is still working properly with the elastic adjusting spool. The simulation result which represents the deformation of each element of the elastic adjusting spool proves that the adjusting spool is now an elastic adjusting spool. Finally, thermal strain equivalent source is added to the Bond-graph model of elastic adjusting spool to develop a thermos-mechanically enhanced one. Then, thermal condition is introduced to the system. At this final stage, the final simulation result represents how the entire system's dynamics is affected due to adding this thermal condition where the control valve is not able to regulate the pressure anymore.

Table of Contents

List of Figures

List of Tables

Nomenclature [1]

A_{in} regulator inlet cross section (m^2)
A_{29} adjusting orifice cross section (m^2)
A_{feed} feedback pipe cross section (m^2)
A_{pis} piston front area (m^2)
A_{pis-b} piston back area (m^2)
A_{drain} drain cross section area (m^2)
A_{out} regulator outlet cross section area (m^2)
b_{tf} transformer coefficient of adjusting spindle (m^2)
c_{tf} adjusting spool front transformer coefficient (m^2)
D_d damping orifice diameter (m)
D_{incs} inlet diameter of adjusting part (m)
D_{feed} feedback pipe diameter (m)
d_{tf} piston front transformer coefficient (m^2)
f_{k-ms} Coulomb friction of control spindle (N)
f_{k-cs} damping device coulomb friction (n)
f_{tf} piston back transformer coefficient (m^2)
h pipes relative roughness
i_{tf} transformer coefficient of plate (m^2)
k_{mss} control spring stiffness $\frac{N}{m}$
k_{63} equivalent adjusting part stiffness $\frac{N}{m}$
k_{tf} internal pressure area of separator $\frac{N}{m}$
l_{feed} length of feedback pipe (m)
m_{mpc} Piston collection mass (kg) 1.14
m_{mss} Control spring mass (kg)
m_{ms} Control spindle mass (kg)
P_i pressure (Pa)
p_i ith element momentum $\frac{kgm}{s}$
Q_i volumetric flow $\frac{m^3}{s}$
q_i ith element displacement (m)
X^0_1 conical surface constant of control orifice start profile angle (m)
X^0_2 conical surface constant of control orifice operating profile angle (m)
x_{ini} control spindle initial displacement (m)
q density $\frac{Kg}{m^3}$
v viscosity $\frac{kg}{m^2 s^2}$
n_{in} inlet loss factor (m^{-4})

n_{fo} first orifice loss factor (m^{-4})

n_{19} equivalent outlet orifice loss factor (m^{-4})

n_{24} equivalent filter loss factor (m^{-4})

n_{48} damping orifice loss factor (m^{-4})

n_{52} drain loss factor (m^{-4})

R_{eq} feedback pipe equal resistance coefficient $\frac{kg}{m^4 s}$

R_{24} filter resistance coefficient $\frac{kg}{m^4 s}$

R_{29} adjusting orifice resistance coefficient $\frac{kg}{m^4 s}$

R_{34} connection pipe resistance coefficient $\frac{kg}{m^4 s}$

R42 control piston friction coefficient $\frac{kg}{m^4 s}$

R_{48} damping orifice resistance coefficient $\frac{kg}{m^4 s}$

R_{52} drain outlet resistance coefficient $\frac{kg}{m^4 s}$

R_{61} damping device resistance coefficient $\frac{kg}{m^4 s}$

$p4$ momentum of inlet flow $\frac{kgm}{s}$

$p20$ momentum of feedback $\frac{kgm}{s}$

$p39$ momentum of control spindle $\frac{kgm}{s}$

$p62$ momentum of adjusting spindle $\frac{kgm}{s}$

$q63$ position of adjusting spindle (m)

$q41$ position of control spindle (m)

1 Chapter 1: Introduction

In this chapter, the background of the thesis project is familiarized in the first part where the goals and motivations of this thesis project is briefly specified, and the structure of this thesis project has been outlined in the second part.

1.1 Project Background

In every space vehicle propulsion system, the hydro control system is the core structure[1]. It includes a thrust regulator, hydraulic control valves and pneumatic complex valves. During space missions, this hydro control system could experience severe internal thermal phenomena that may be catastrophic for a typical liquid space engine if not identified. Thermal conditions involve the dilation of the valve's internal components, known as spools, and material softening due to the rise in temperature. Such thermal expansion in a valve's components can induce undesired dynamics in the system and change the operational set-points of the control device. Additionally, material softening may change the response modes of the entire control system. These unwanted changes in the system's behaviour may result in failure of the space engine's hydraulic circuit by initiating destructive disturbances and making the entire system unstable[2]. A thorough investigation on hydro control system to thermal impacts is the objective or goal of this thesis.

To achieve this aim, it is very important to add thermal domain dynamics into the existing multi-physical system on which the investigation of thermal impact will be performed. In such multi physical system, the dynamics of thermal phenomena are not explicitly visible [3]. Therefore, to carry out this investigation, a physical way of modelling which can vividly expose the non-linear dynamics of thermal phenomena while interacting with the subdomains of the system is required. It is expected that by using such method, the physical dynamics like structural dilation or viscoelastic damping can be addressed through the basic physics which govern the behaviour of the system. Considering all these aspects, Bond-graph method has been chosen for this thesis which working principle is based on the continuity of power within multi-physical system.

1.2 Outline of This Thesis

In this thesis, an investigation on thermal impact on space vehicle hydro control system has been carried out by means of Bond-graph physical approach of modelling. The outline or structural layout of this thesis is as followed:

In chapter 2, a comprehensive study of literatures associated with different methods of investigating true physical dynamics of hydro control system under thermal conditions has been presented. Besides, comparison among different methods has been performed by analysing them which has revealed Bond-graph as the most suitable method to applied here in this thesis.

In chapter 3, the proposed Bond-graph technique has been discussed in detail where Bond-graph representation with its fundamental elements has been introduced. It has also been demonstrated how Bond-graph approach deals with multi-physical domain system with non-linear interactions. Specifically, Bond-graph method for mechanical system and hydraulic system has been illustrated in this chapter. One of the of most important tasks of extracting mathematical model of the system from respective Bond-graph model has also been discussed here.

In chapter 4, the existing pressure control valve which is the system of concerned has been remodelled as this is the first and most significant goal of the thesis. This remodelling involves modification in adjusting part of the control valve. This chapter represents why this remodelling is required and how it has been achieved using Bond-graph technique and finally, the physical dynamics of the remodelled system has been analysed to make sure that the remodelled system is performing better than the original system.

In chapter 5, one of the rigid moving elements of the remodelled pressure control valve which is adjusting spool has been replaced with the elastic adjusting spool in order to investigate the thermal condition as with rigid spool configuration, thermal dynamics cannot be captured. At first, the Bond-graph model of the elastic spool has been achieved and then incorporated into the Bond-graph model of the control valve, obtained in chapter 4. At this stage, the mathematical model of the system with elastic adjusting spool has been extracted from that respective Bond-graph model. With the help of mathematical model, simulation has been performed and results have been discussed with proper critical analysis.

In chapter 6, the elastic adjusting spool has been thermo-mechanically enhanced which has made the elastic spool capable of addressing thermal phenomena such as structural dilation. To do so, at first the Bond-graph model of the thermo-mechanically enhanced spool has been derived by adding that extra feature (mechanical strain) to the existing elastic spool. Then, thermal condition has been added to the system and the obtained simulation results at this stage has revealed the unwanted dynamics of the system due to the thermal condition.

In chapter 7, significant conclusions, presented in this thesis based on simulation results, have been drawn with proper recommendation.

2 Chapter 2: Literature Review

In this chapter, contemporary literature associated with investigation of thermal impact on space vehicle hydro control system has been critically reviewed. At first, all significant consequences related to thermos-mechanical phenomena in hydro-control system have been discussed in this chapter. Then, different types of techniques, applied to investigate the physical behaviour of such control device, have been studied, through which it has been crystal clear why Bond-graph approach of modelling is feasible for this thesis. Therefore, Bond-graph technique in modelling physical dynamics of such system has been used in this thesis. Through this literature review, the capability of Bond-graph approach in investigating thermal impact on hydro-mechanical system has been demonstrated.

2.1 Review of Consequences of Thermo-Mechanical Conditions:

During the operation of the control valve, an unwanted dynamic has been observed recurrently due to the thermal dilation of valve's component (spools). The shrinking or expansion of control valve's component largely depends on the heat exchange occurring between the flow and the valve's internal component and the factors on which heat exchange depends are- the magnitude of temperature and the velocity of the internal flow. Due to this thermal dynamic, the size of control cavity inside the valve can be changed which may lead to deviations in set-points of the system, the key control parameters. In addition, changes in the physical geometry of the control valve such as structural dilation and material softening are noticed because of the heating and cooling mechanisms. Thus, alteration of material properties such as material softening (stiffness) of the spools co-occurs with the dilation of valve's component. In such condition, an unwanted internal noise is induced due to the transmission of turbulent frequency in the valve's spools structure as per the level of induced cooling or heating mechanisms. This induced noise has an adverse effect on system's transient performance that may cause severe explosion by destabilizing the whole system. Therefore, to achieve successful operation of space vehicle hydro control system, investigation of these thermal dynamics and understanding their behaviour are very important and this is the first step towards the designing of a control strategy to suppress them.

2.2 Study of Different Methods Used to Investigate Physical Dynamics (thermomechanical conditions) of the System:

There are certain different approaches that have been used for investigating thermo-mechanical phenomena of any structure such as Finite Element Method (FEM), Finite Volume Method (FVM), Finite difference Method (FDM), Transfer function approach, and Bond Graph (BG) Technique [4]. FEM is one of the most commonly used numerical approaches that solves problems with coupled

thermo-elasticity. In a study of Odon and Kross, an overall concept of FEM has been discussed where the purpose of using this method was capturing the thermomechanical phenomena as precisely as possible by performing the discretization of the continua [5]. However, the time cost to generate the models using this FEM was unexpectedly high. Besides, the models built in such manner might not be the appropriate ones in terms of the control aspects because the result is a nonlinear algebraic problem with enormously higher-order numerical values. As per control aspects, a desirable method of modelling is one that can generate comparatively lower-order and analytical models within the real-time frames. Apart from being capable of investigating system's inherent dynamics, the resultant models should be simple or easier enough to be implemented in derivation of control laws. Considering all these aspects, however the outcomes of FEM naturally failed.

Another effective method is transfer function method which has been used by Ray and Watton to analyse the dynamics of a single stage pressure relief vale where quite a few modifications have been carried out by them[6] [7]. Later on, this transfer function approach has been implemented by Yung C for capturing both the static and dynamic behaviours of a two stage pilot relief valve[8]. In this study, it has been observed that the applied transfer function method was capable of addressing the dynamic behaviour of the system within a certain degree of operating point. However, the linearization system of this approach was not able to investigate the integrative dynamics inside a multi-physical domain set up which is a highly non-linear system. Additionally, the resultant models of this method were unable to represent the exact physical meaning of the underlying thermo-mechanical conditions. For instance, to represent physical dynamics like thermal expansion which is the consequence of the interactions between two different subdomains, the models of the system are desired to have strong relation with the subdomains structures and parameters along with the nonlinear interactions among different subdomains.

Considering the dynamics and characteristics of multi-physical domain systems (hydraulic system and thermomechanical system), the most suitable technique, based on the energy flow exchange is the Bond Graph (BG) technique [9] [10] [11]. The detailed explanation of this BG method along with its applications has been reviewed by Karnopp and Rosenburg seamlessly [12]. This technique has a diagram based tool which is quite effective for describing any physical system inside the system's subdomain settings and predicting the respective characteristic or behaviour of the physical system of concern [13]. As the models developed by BG method are consisted of its subdomain's models which are internally connected based on the conservation law of energy and power exchange [14], the resultant models are recognized to be reusable and physical to demonstrate the interactive behaviour of a complex system with multiple domains [15].

2.3 Bond-graph (BG) Technique in Modelling Hydraulic system and Investigating Thermo-Mechanical Phenomena:

There are several publications [1] [16] [17] where the application of BG technique in modelling and simulation of hydro control valve's dynamics is studied meticulously. These studies are mentioned the significance of modelling such regulators or control valves regarding their high sensitivity in property changing behaviours such as structural dilation and material softening considering the true physical meaning of any specific issue. Additionally, as per [1] [16] [17], to model these control valves with accuracy, the mathematical approximations have been avoided and the valve's sub-systems have also been modelled following the same technique. They have discussed some strong reasons for using BG method for modelling and simulation of the non-linear dynamic behaviour of such control valves where one of the major advantages was the ability of BG technique of extracting the smaller independent equations of system's dynamics with perfection. As BG method represents the physical way of modelling, the results obtained with such method are suitable for a wide range of system's dynamic behaviour. Another main advantage that has been emphasized in here, is its capability of modelling higher-order non-linear systems with several inputs and outputs. Most of the studies on hydro-control valves therefore have been reflected the use of BG technique for modelling and simulation of the system's dynamics. In all those literatures, to avoid the unwanted impact of thermal conditions in valve's system's dynamics, a rigid spool assumption was considered. However, the models produced using BG technique were non-linear and analytical which can provide a wide range of dynamics of such multi-physical systems, these models were integrally unable to represent the real-life aspects due to the violation of rigid-spool concept. Physically, the induced thermo-mechanical phenomena inside the system has a direct and adverse effects on the rigidity of the spool that make the models vulnerable under thermo-mechanical conditions. Consequently, the valve's system becomes inevitably susceptible in passing through the operational frequency and unreliable in real-time operations. Therefore, later on studies have been carried out where the assumption of rigid-spool was eliminated [3]. In this paper, Amir and Fangpo have proposed an elasto-expansive model of the spool using BG method so that this can be incorporated into the existing valves models, built in terms of BG method. According to this study, by replacing the rigid-spool of the control valve with the elasto-expansive one, the thermo-mechanical conditions of the system can be controlled as the proposed thermo-elastic model of the spool is able to investigate the coupled effects of structural dilation and the softening of material of the spool as well. Moreover, the true physical understandings of system's dynamics can be provided by introducing this BG elasto-expansive model of the spool. In this study, at first a distributed elastic model of the valve's spool was produced using BG technique where identification of every possible adjustments or additions were performed for addressing the ultimate thermo-mechanical conditions.

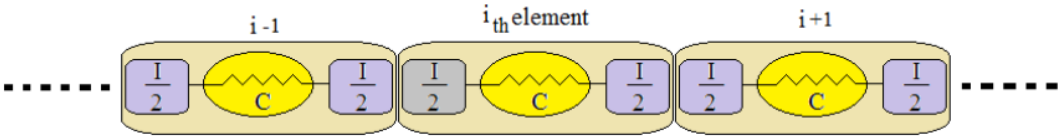

Figure 1: 1D beam reticulation[18]

In Fig. 1, a simple Rayleigh reticulation of a beam structure has shown where each element has been configured by two different types of storage elements, inertia(I) and capacitor(c). The storage elements, inertia and capacitor represent the kinetic energy and potential energy respectively where the first element (I) has distributed at both the ends on the boundary and the second element (c) has considered as the centre element. Thus, the potential energy has been stored at the centre of each element in the reticular space and the kinetic energy has been stored at the boundary of that element. The desire BG model of the discrete beam in Fig. 1, has been shown below from where the state variables for i_{th} element and j_{th} junction have been derived as per the conservation of energy.

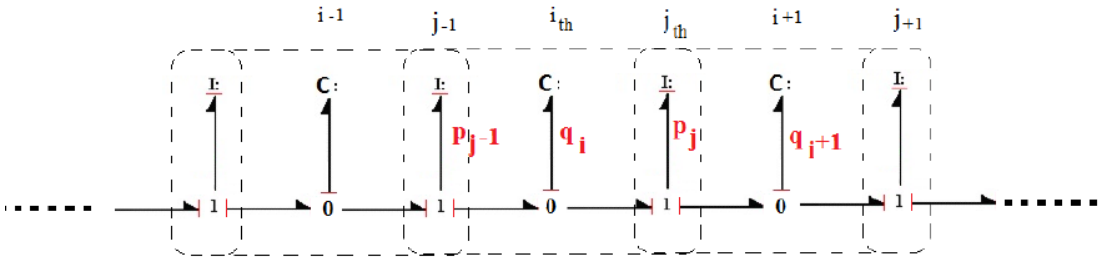

Figure 2: BG model of the elastic model[18].

Then, the effect of structural dilation was investigated by adding a thermal load to the elastic model of the spool which referred the behaviours (dynamics) of the structural dilation [18].

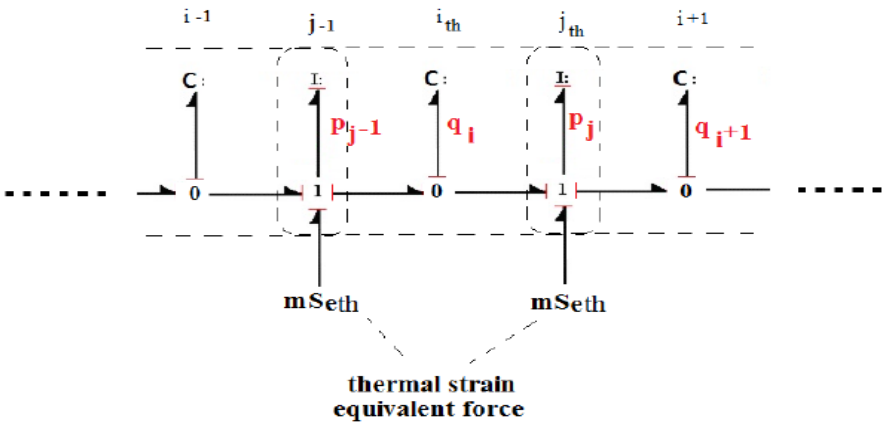

Figure 3: BG model of the elasto-expansive beam[18]

In Fig. 3, the BG model of the expansive spool has been shown with the injected thermal effort derived from the new state equation.

To address the another effect of thermal condition which is material softening, a new modulated storage element was added to the elastic model to replace the traditional constant storage element as the new modulated storage element was able to provide the effect of changing elasticity due to the induced temperature[19]. After injecting the thermal effort in the existing BG model of the elasto-expansive spool, the resultant BG model (Fig. 4) was able to reveal the thermal information of the system.

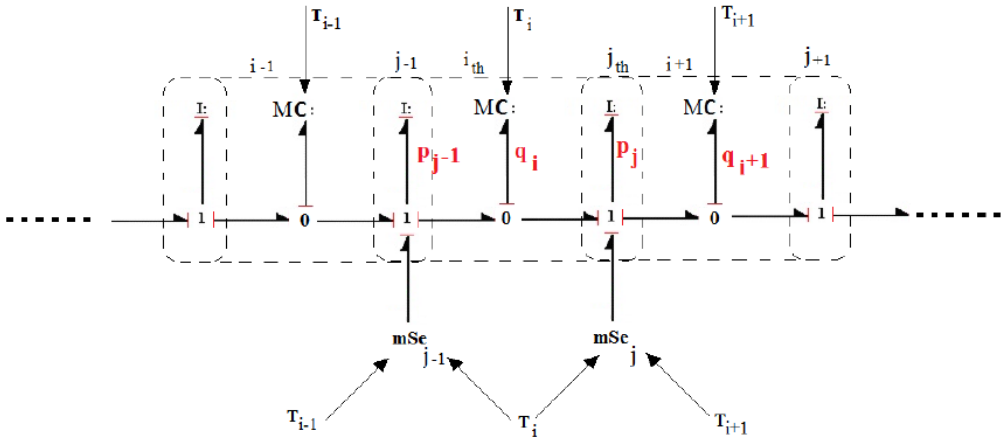

Figure 4: BG model of the thermo-mechanically enhanced beam with material softening and structural expansion characteristics[18]

The Fig. 4 of thermo-mechanically enhanced spool represents that the thermal condition has been injected to both the capacitor and inertia through a single port of the storage element and the energy port of the momentum junction. Thus, the resultant BG model represents the changes in system's dynamics due to the thermo-mechanical conditions in a single elastic domain.

2.4 Bond-graph (BG) Technique in Modelling Domain-independent Conduction Discrete Model to Investigate Multiple Domain's Dynamics:

In a recent study of [20], the BG approach of modelling system's physical phenomena has been implemented to build a domain independent conduction discrete model for investigating multiple domain's dynamics. According to this paper, to represent the nonlinear behaviour of a thermal subdomain in a coupled multi-physical system, a physical way of modelling is required as the thermal subdomain is not clearly visible. Additionally, to unveil the interactive multi-physical conditions like

viscoelastic damping and material softening, a port based method considered as BG method needs to be implemented as the BG method is based on power continuity inside system's dynamics [21]. In this paper[20], Amir and Fangpo have attempted to fill the gap between a theoretically modelled thermal conditions of the system and its realization in a multi-domain physical system by a discrete geometry that reveals geometric compatibilities of the system of concern. A nonlinear 1-D conduction model has been proposed here in this study associated with the investigation of thermos-elastic dynamics. With the help of BG method, the true physical characteristics of the domain-independent conductive discrete component can be addressed explicitly. This paper has also discussed on how the compatibility reflections of the concerned model can deliver the proper direction to form the bridge between thermal and elastic subdomains. As per this paper, initially, a 1-D conventional heat conduction model has been built applying BG method where the BG representation contains a chain of energy components such as dissipative, R and capacitive, C elements, showing in Fig. 5 [20]

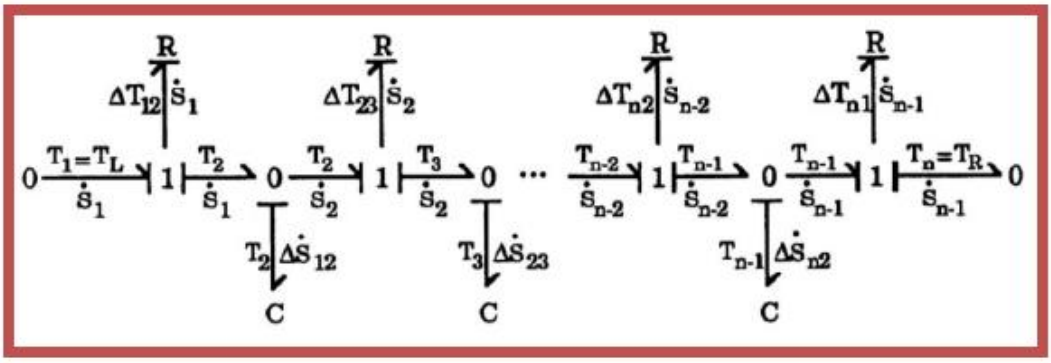

Figure 5: BG model of conventional heat conduction [20]

With this BG model, it was found that the energy dissipated by the resistors were going nowhere which indicated that considering the heating of the system, this model did not make sense while the system itself was in the thermal domain. Then, to solve this problem, each of those resistors were replaced by as RS component which is a resistive source and can produce entropy to be re-injected into the existing subdomain. The modified BG model has shown in Fig. 6.

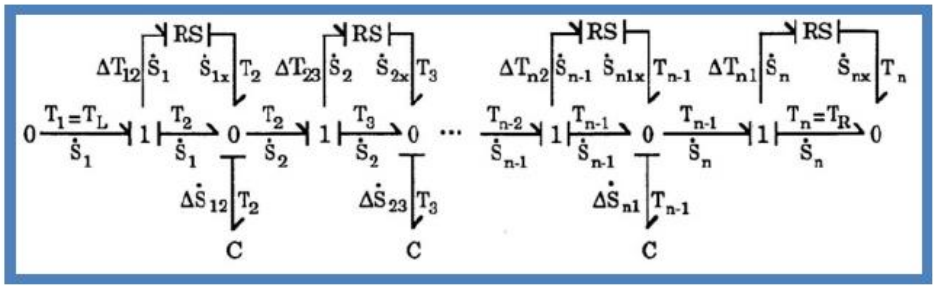

Figure 6: Modified BG model of conventional heat conduction [20]

After producing this BG model, the compatibility considerations of the system's component were generated to make this BG model working for the coupled multi-domain physical system. The configured schematic of 1-D heat conduction element is as followed.

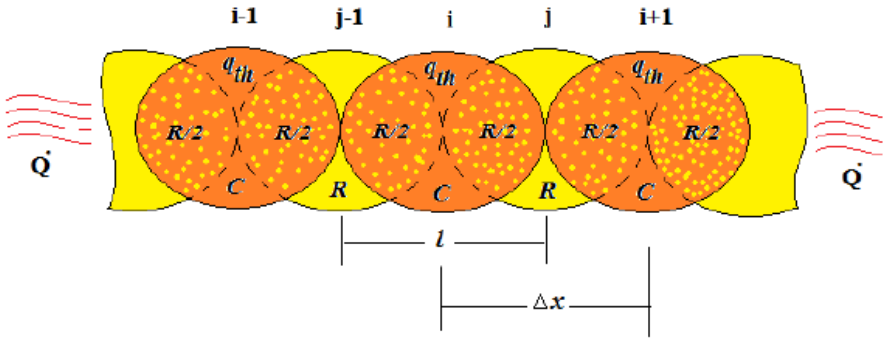

Figure 7: Schematic of 1-D heat conduction[20]

According to this schematic, the way thermal energy was stored in one side and dissipated from the other side of the component, it was difficult to obtain power divergence information from such conventional model. Therefore, each of the compoments of the system was considered to be dissipative and energy storage components so that the proposed thermal component can be generated. The obtained BG model of Fig. 7 with respect to dissipative components and materials properties of each component has attached below.

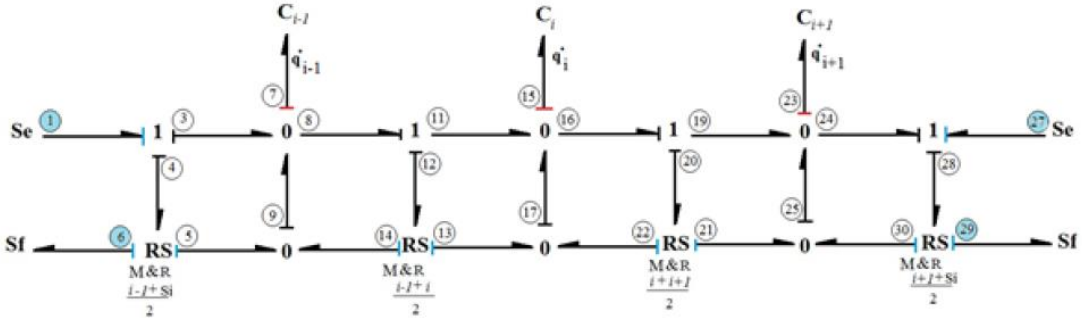

Figure 8: BG model of 1-D conduction[20]

This BG represtation of 1-D conduction reflects that each element of this model is configured as C storage element along with the state variable (q_{th}) that represents the stored entropy. Here each, C element is connected to the adjuscent element by two junction elements. A complete connectivity between the thermal and elastic subdomains is as followed.

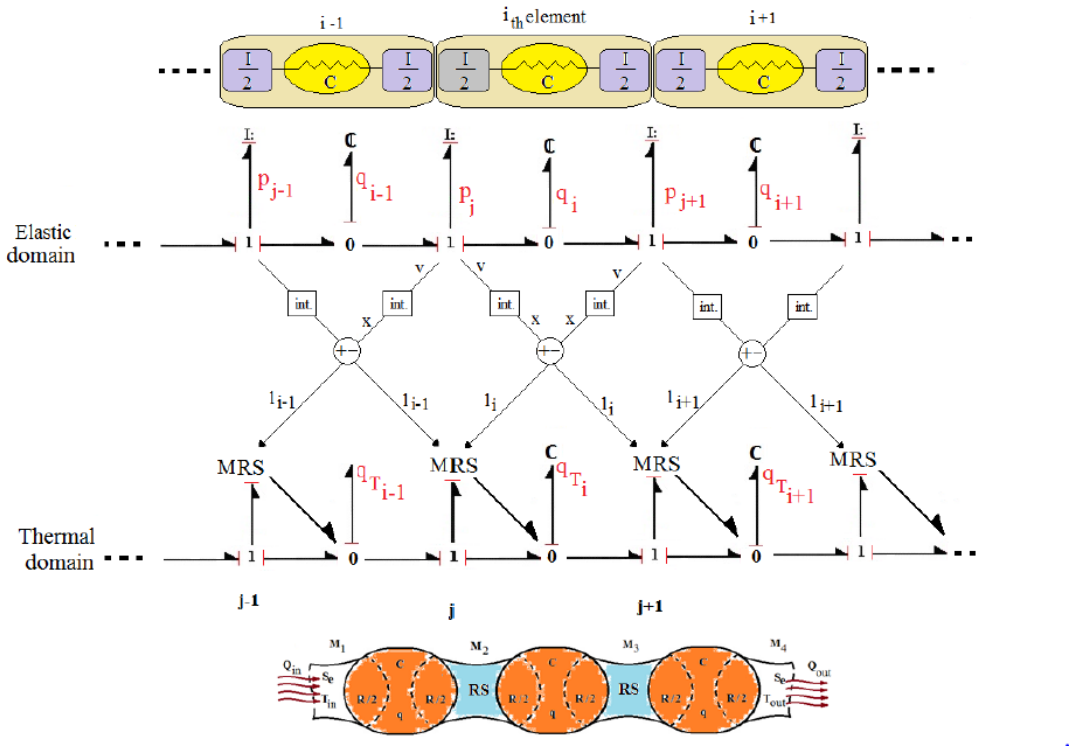

Figure 9: Geometrical connections between elastic domain and thermal domain[20]

Thus, to investigate the multi doamin physical system's dynamics of heat conduction, a domain-independent thermal component based on energy configuartion has been introduced in this study. This configuration has been proved as a very strong tool in such multi-domain physical system for examining overall system's dynamics. Therefore, it can be stated that BG method is undoubtedly an effective way of modelling physical dynamics of multi-domain systems.

To conclude, the early literatures reveal different methods of modeling and simulation of nonlinear physical system such as FEM and TF methods where the resulatnt models were unable to capture the system's dynamics in a wide rang of control aspect. Studies related to these methods also reflect that the models obtained using such methods were not analytical within real-timeframe and therefore, the true physical meaning of the induced thermo-mechanical conditions was not achieved. In early 1980's, a physical way of modeling which is BG technique was introduced to model control valve in hydro control system where interactive system's dynamics were modelled and simulated in multi-physical domain-settings. Models produced using BG technique are able to provide true physical meaning of system's dynamics and from the BG model, the real state variables can be extracted following the Bond graph rules for extracing mathematical equations [22]. After obtaining the state space equations of the system, the dynamic behaviours can be analyzed via simulation method. BG method therefore is the most suitable and poweful tool to model and simulate any multi-domain physical systems.

3 Chapter 3: Introduction of Bond-graph Technique

3.1 Bond-graph Representation

A Bond-graph is a physical method of modelling any dynamic system consisting of multiple subsystems, components or fundamental elements which interact through energy exchange. A Bond-graph can fundamentally represent any discipline, including mechanical, electrical, and hydraulic. It facilitates the conversion of that system into a state-space representation, meaning that systems from various energy domains can be modelled in the same fashion. Unlike block diagrams, the Bond-graph approach denotes the bi-directional exchange of energy. The Bond-graph approach is fundamentally domain-independent, and thus is a very convenient tool to incorporate multiple domains. The generated sub-models from a Bond-graph approach are reusable, as models obtained using this method are effectively non-causal. The Bond-graph approach is an object-oriented form of modelling physical systems[23].

The concept of this physical approach was originated by Paynter in 1961. It was further improved by Karnopp and Rosenberg, as described in their textbooks published in 1968, 1975,1983 and 1990. According to their study it is a highly practical technique (Thoma, 1975 & Van Dixhoorn, 1982). In 1984, a framework that implemented the Bond-graph method with thermodynamics was demonstrated by Breedveld, using formulation [24].

Bond-graph example:

In this method, “bonds” connect different types of elements with single port, double port and multi-port, and each bond presents the instantaneous flow of energy or power. Power variables are used in the Bond-graph to represent the flow of each bond. This power variable is invariably represented as a pair of flow and effort.

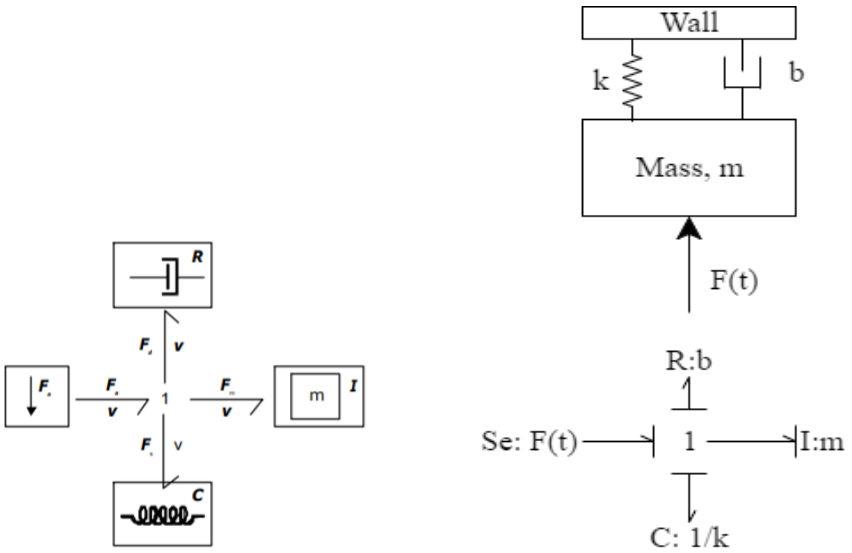

Figure 10: A simple system with mass-spring-damper and its respective bond-graph model with mechanical symbols (left) and standard symbols (right)[24].

In the above Figure, a mechanical system with damped mass-spring is shown for two port variables of the Bond-graph elements. The variables are: the force on the element port and the velocity of the element port. For rotational mechanical system, the port variables are torque and angular velocity. The power here is the product of the force and velocity which can be exchanged via a port with the remaining parts of the system. According to Newton's law for a free body mass diagram,

$\sum F = -Fb - Fk + F$ where $\sum F = m\dot{v}$

From the above figure, all the loose ends have same velocity, denoted by v . At junction 1, the sum of the forces is zero according to the sign of power direction. Here, force is equivalent to the effort and velocity is equivalent to the flow. In the case of a rotational mechanical system, torque is equivalent to effort and angular velocity is equivalent to flow. This indicates that force is analogous to electric voltage and velocity to current. The analogies between the mechanical and electrical elements are followed:

- Damper (b) is analogous to the resistor (R).
- Spring (1/K) is analogous to the capacitor (C) which is the mechanical compliance associated with electrical capacity.
- Mass (m) is analogous to the inductor (I).
- Force (F) is analogous to the source voltage (Se=Source effort).

The velocity is analogous to loop current.

Bond-graph Elements:

The basic elements of Bond-graph are as follows:

R- is the resistor, dissipating free energy e.g. mechanical friction or electrical resistor

C- is the storage element for a q type variable e.g. spring, stores displacement

I - is the storage element for a p type variable e.g. mass, stores momentum

Se and Sf - are sources e.g. voltage source in electrical system and flow source in hydraulic system

TF – transformer in electrical system and lever in mechanical system

GY – gyrator or electromotor in electrical system and centrifugal pump in hydraulic system

0 1 junctions- for connecting two or more sub-models in a Bond-graph

3.2 Causality of Bond-graph Method

The Bond-graph method's causality determines the direction of each bond's signal flow, where the bond is assumed to be bi-directional [23]. After performing a causal analysis, the resultant model is a causal Bond-graph that is considered to be a complete block diagram. Causal analysis is the most important task when using the Bond-graph method to extract mathematical equations, because it provides an accurate visualisation of the obtained model. Based on the type of equations, constraints can be imposed on the associated bonds by the element ports. There are four types of constraints that should be considered before performing causal analysis of the Bond-graph method [25]. They are discussed below.

Fixed Causality:

Fixed causality defines a state where only one port variable will be allowed to be the outgoing variable between two of them by the equations. It happens at sources, for example, the effort source (Se) has fixed causality which means that it always has its effort to be the outgoing signal and a causal stroke directed to the outwards. This effort source causality is known as effort-out causality and similarly, for flow source (Sf), this is known as flow-out causality[23].

There is another state at non-linear elements where fixed causality happens. For example, the basic Bond-graph elements: R, GY, TF, C, and I where fixed causality can be imposed for two different reasons. They are-

- Due to not having any relation between port variables and
- The equations being singular or not invertible.

Constrained Causality:

Constrained causality happens where there is a relation between the causalities of the port variables of different elements. For example, TF, GY, 0 and 1 junction, as the causality of any one port imposes

here the causality of another port. In case of TF, between two ports, one has effort-out causality and other has flow-out causality. For GY, both the ports have either effort-out or flow-out causality. As the 0 junction is the common effort junction, so one bond must take the effort in which denotes that 0 junction always should have only one causal stroke at junction side. For 1 junction, as all the flows are same, so one bond must take the flow in which means that there should be only one bond with stroke away from the junction[23].

3.3 Bond-graph for Modelling Hydro-mechanical System

Constructing the bond-graph model for hydro-mechanical system can be explained into two different stages. In one stage, construction of Bond-graph model (physical model) of mechanical system will be discussed and another stage will be involved of Bond-graph modelling of hydraulic system. Following table shows different Bond-graph variables for different energy domains.

Table 1: Bond-graph variables for different energy domains[23]

Energy-Domains	**Effort (e)**	**Flow (f)**	**Generalized Momentum (p)**	**Generalized Displacement (q)**
Translational Mechanics	Force (F) [N]	Velocity (v) [m/s]	Momentum (p) [Ns]	Displacement (x) [m]
Hydraulic domain	Total pressure (P) [N/m^2]	Volumetric flow (Q) [m^3/s]	Pressure momentum (Pp) [N/m^2s]	Volume (Vc) [m^3]
Thermodynamic	Temperature (T) [K]	Entropy flow ($\dot{S}$) [J/K/s]	_	Entropy (S) [J/K]

Bond-graph modelling of mechanical system:

The starting point for building of Bond-graph model for mechanical system includes distinct velocities and angular velocities.

- At first, the distinct velocities and angular velocities of the system need to be identified to configure them via 1 junction. In order to identify which 1 junction express which velocity

(flow), they must be denoted by a particular name. For instance, the ground is usually denoted by a 1 junction that has zero velocity (flow) source (Sf).

- Then, in a 0 junction, 1-port needs to be connected with C energy element which is for mechanical springs and 1-port needs to be connected with R resistors element which is for dashpot. These elements must be inserted to the 0 junction which is between two 1 junctions as shown in figure attached below. The sysmol 'X' can be represented either by C element or R element as mentioned above. To, express the velocity difference at the port, in 0 junction, one bond must be directed towards the 0 junction and one must be pointed away the 0 junction.

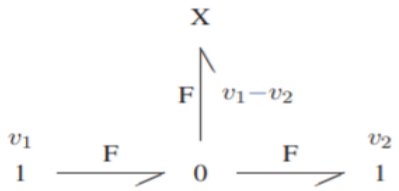

Figure 11: Sprigns (C) or dampers (R) between two different velocities (v1 and v2)[23].

- 1-port inertia elements (I) should be inserted to their associated 1 junction. As in case of rigid component, the motion of the centre of gravity with respect to a fixed axis is considered as the reference to an inertial frame. Kinetic energy of the rigid body (stored by I-element) directly attached to the 1 junction which denotes the velocity or angular velocity.
- Then 1-port sources and 1-port sinks should be inserted to the respective 1 junction where sources and sinks defines the boundary conditions. For example, every mass or body is subjected to the gravity force. As 1 junction denotes the sum of all forces or moments acting on a body, sources or sinks are directly connected to the appropriate 1 junction.
- In this step, orientation of bonds is required to perform. With the insertion of all elements to the Bond-graph, directions of flow of energy are assigned to the bonds. Therefore, it is required to consider empty energy stores with an energy flow from sources via the junction into energy stores or sinks. Thus, orientation of bonds must be done following the rules that have been already mentioned for each element of the Bond-graph. Specially, orientations at 0 junctions attached to the power port of the C element (energy store) or R element must represent a velocity difference as shown in above figure.
- In the last step, simplification of the Bond-graph should be done which includes condensing of two junctions of same type either 0 junction or 1 junction into a single junction. The following figure (a) represents how two same type of junctions can be condensed into a one junction where symbol 'J' can be either a 0 junction or a 1 junction.

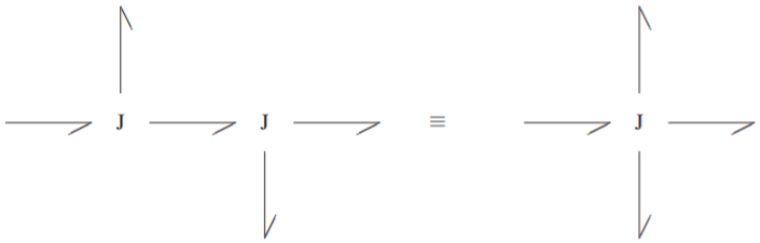

Figure: (a)

Another simplification is replacing 2-port junctions along with through representation of adjacent bonds by a single bond as shown in the figure (b) attached below. This simplification can be done only if the both adjacent bonds of a 2-port junction possess inward configuration.

Figure: (b)

By doing such condensing, the sign of one of the 2 power conjugated variables can be changed. The following figure (c) with 0 junction shows the corresponding sign change.

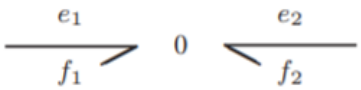

Figure 12: Sign change at a 2-port junction, $f2 = f1$ [23]

In the Bond-graph of any mechanical system, 2-port junctions with inward configuration at adjacent bonds usually used to clearly denote the internal forces in a body appeared in free body diagram. In general, it has been recommended to add labels to all the elements in Bond-graph to identify them easily and differentiate from other elements of same nature[23]. Each label defines a parameter or sometimes a function of parameters in Bond-graph.

Bond-graph modelling of hydraulic system:

- For Bond-graph modelling of a non-mechanical hydraulic system, at first all the distinct efforts are required to be identified and configured by 0 junctions. Which means that as per Table 1, the absolute pressures in hydraulic systems can be represented by 0 junctions. Similar as 1 junction in Bond-graph for mechanical systems, all of them (pressures) need to be labelled with a name to be differentiated from other elements of same nature.
- The power port of any non-mechanical system like hydraulic system, is an energy store. Such energy stored power port like a resistor, a 2-port transformer, a 2-port gyrator or a source should be connected to the 1 junction which has to be inserted between appropriate pair of 0 junction.

For example, in the electrical transformer there is two 1 junctions at both port of the transformer that denotes the currents passing through the transformer windings. In case of hydraulic system's Bond-graph, C elements usually need to be connected to a 1 junction placed between two 0 junctions which respectively represents the absolute pressure and atmospheric pressure. The figure attached below shows the Bond-graph of the 2-port transformer element and single port C element.

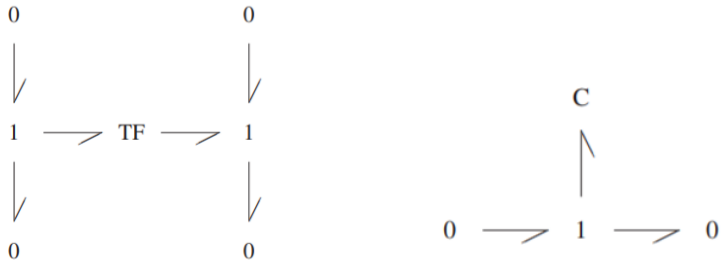

Figure 13: Insertion of a 2-port transformer element and single port capacitor element with the direction of flow of energy[23].

- After inserting all the required elements, the directions for flows of energy are needed to be assigned considering that empty energy store and flows from the sources to the dissipators or sinks via the junctions. Considering this interpretation, configurations of bonds have to be implemented as per the rules already mentioned for all Bond-graph elements[25].
- For hydraulic systems, the atmospheric pressure of return tank is usually chosen, and the associated 0 junction of this pressure has been eliminated with all adjacent bonds. With the new configuration, the 0 junction shows the gage pressure. Thus, simplification of Bond-graph representation has been obtained in hydraulic system. In such case, as 0 junction is the configuration for gage pressure, the C elements must be connected directly to the associated 0 junction. Additionally, since the transformer elements for the hydraulic system Bond-graph define a pressure to its corresponding mechanical force and also define the volumetric flow of the incompressible fluid flow to its corresponding translational velocity, the hydraulic port for the transformer element has to be attached at 0 junction that represents gage pressure and the mechanical port has to be attached at 1 junction that represents velocity[25].
- Finally, simplification of the Bond-graph can be done using condensing method as has been explained for the mechanical system in the first stage. Besides, it is always a good exercise to insert labelling for all the elements in order to differentiate them from other elements effortlessly[25].

3.4 Extracting Mathematical Model (state equations) From the Associated Bond-graph Model

As the obtained Bond-graph model possess causality, the information about order of the set of state equations can be achieved by causal analysis. While assigning causality on the Bond-graph, one of the preferences include the number of storage elements that have integral causality, equals the number of initial conditions. This number defines the order of the entire system and the order of the set of state equations can be equal or less than that of the system as some storage elements of Bond-graph are dependent on each other. Such type of storage elements together denotes one state variable whereas they have their own initial conditions[23]. The following Fig. 14 represents a system with order two where there is a factor in between input signals.

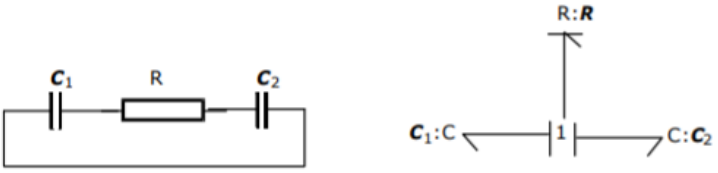

Figure 14: System with higher order than the order of the state equations where causality has been assigned with integral causality.

A causal Bond-graph contains all necessary information required to extract mathematical model or set of state equations. The set of state equations can be either ordinary first order differential equations (ODEs) or a set of differential and algebraic equations (DAEs)[24]. Models with ODEs do not have any causal conflicts as they explicit in nature whereas models with DAEs are implicit with causal conflict[24]. In this thesis project, the set of state equations are ODEs. However, there are Bond-graph software such as Enport (Rosenberg, 1974), MSI (Lorenz, 1997), CAMP (Granda, 1985) and 20-SIM (Broenink, 1990, 1995, 1997,1999)[24], in this project, the state equations have been extracted by hand. Therefore, the process of generation of state equations by hand is discussed here.

- At first, the set of all algebraic and mixed differential equations have been written down. As these equations represent the constitutive connections among all Bond-graph elements in computational form, this contains 2n number of equations of a Bond-graph with n number of bonds. Out of 2n equations, n equations calculate an effort and n equations calculate a flow or derivatives of effort or flow.
- Then elimination of algebraic equations has been done. As the equations are being generated here by hand, the very first step of elimination must be taken into consideration. The first step of elimination involves formulations of equations by, at the sources, where the signal function has been used directly at the bond. Then, the variable determining has been written to the associated junction along all bonds those are connected to that junction. This junction defines

that variable which has been assigned to bond variables using the identity of the junction. For example, at a 0 junction, the only bond having its causal stoke towards the 0 junction, represents the effort of that junction. Similarly, at 1 junction, the flow of that junction is defined by the only bond having its causal stoke away from the1 junction. In chapter 4, the extraction of mathematical equations for the proposed pressure control valve have been discussed elaborately.

3.5 Simulation Model of the Respective Bond-graph Model:

Simulation model of a Bond-graph representation can be defined as the resultant set of state equations extracted from the respective Bond-graph model of the system. As it is consisted of first order differential equations (ODEs), simulation can be done using standard numerical integration methods[24]. Besides, the numerical integration is an estimate of the real integration method, the simulation model therefore, needs to be checked on aspects important for simulation[24]. Thus, a proper integration method needs to be chosen where the computational work is less, and the result of simulation is valid for a wide range within an acceptable margin of error.

For causal analysis, the obtained Bond-graph model can be changed in order to develop an explicit simulation model. So, it is always a good practice to consider the consequences of simulating the relevant dynamics of the simulation model. Few aspects related to the simulation with a numerical integration method have been discussed here.

- Implicit equations:
  Algebraic constraint equations (DAEs) are known as implicit models which can be simulated only with implicit integral method. However, the explicit models with ODEs can be simulated using either implicit integral method or explicit integral method[24]. So, causal analysis plays an important role here as it can reveal the nature of simulation model about being explicit or implicit.
- Discontinuities:
  When, integration method with distinct requirements is not available, variable step process can be implemented. However, multistep process has less accuracy as they require previous information and thus discontinuity occurs[24]. Therefore, it is important to mark the presence of discontinuity while modelling the system.

4 Chapter 4: Remodelling of the Pressure Control Valve

4.1 An Overview of the Proposed Hydraulic Control System

In a space vehicle propulsion system, the hydro control system is the heart of propulsion system, and consists of thrust regulators, control valves and pumps. There is no alternative system that can maintain flawless valves and thrusters like pressure control valve for the control of propellants and pressures. It assures the highest possible reliability and performance of the space vehicle. The range of such control valves involves:

- Flow control valves for both monopropellant and bipropellant thrusters.
- Pressure regulators.
- Low flow latch valve.
- High flow latch valve.
- Pyrotechnic valve.
- Fill, drain and vent valves for propellants and gases.

This thesis project investigates the pressure regulators as a major component of hydro control systems. In hydro mechanical systems, the modelling and simulation of such regulators are typically performed to investigate any feasible behaviour of the systems. Current research has largely focused on simulations of the dynamic behaviour of regulator valves. In the proposed valve, pressure fluctuation is controlled or regulated by changing the cross-section area of the flow. However, the simulation process in such pressure valves is not straight forward due to complexities caused by simultaneous fluid acceleration and moving mechanical parts.

Previous researches use mathematical assumptions to represent that the simplification of those complexities. It must be noted that such assumptions can affect the accuracy of simulation outcomes. This limits the suitability of the obtained results. It is therefore essential to avoid mathematical approximations as much as possible and consider all the physical aspects of the valve while modelling.

4.2 Physical model of the control valve (pressure regulator):

The pressure regulator proposed in this study is a typical indirect hydro control valve that is widely used in space launch vehicle propulsion system. Fig. 15. shows a sample type of this pressure regulator indicating the four main segments of such control valves. There are two main types of dynamic subsystems associated with this pressure regulator, namely the mass spring and hydraulic system. The four major components of this regulator mentioned in the following figure are[1]:

(a) Control section

(b) Amplifying section

(c) Adjusting section

(d) Pre-adjusting part & damping device

A simplified schematic of this pressure regulator has been shown in Figure 16, with all valve components represented precisely. According to Fig. 15. the control section, shown in section (a), is comprised of inlet, outlet and control orifices. In this section, the control orifice's cross-section area is changed by the movement of a control spindle or spool. Section (b) is the amplifying section, consisting of the control piston, rod, damping orifice and course constraints. This section carries out the amplification of the pilot-signal, which is regulated by the adjusting section. The most sensitive segment of this valve is section (c), the adjusting section, consisting of the adjusting spindle, flexible components, feedback-path, adjusting orifice and placoid. In this segment, once the imposed perturbation is sensed, the command for the control section is controlled and sent. All types of control valves like the proposed one, have a pre-adjusting section (d) that is controlled manually via an adjusting screw. The noise of the system is restrained using coulomb friction to mitigate any issues with the high-pressure range operation of such control valves and their adjusting sections' minor courses. Thus, potential for unexpected motion of the system is reduced[1].

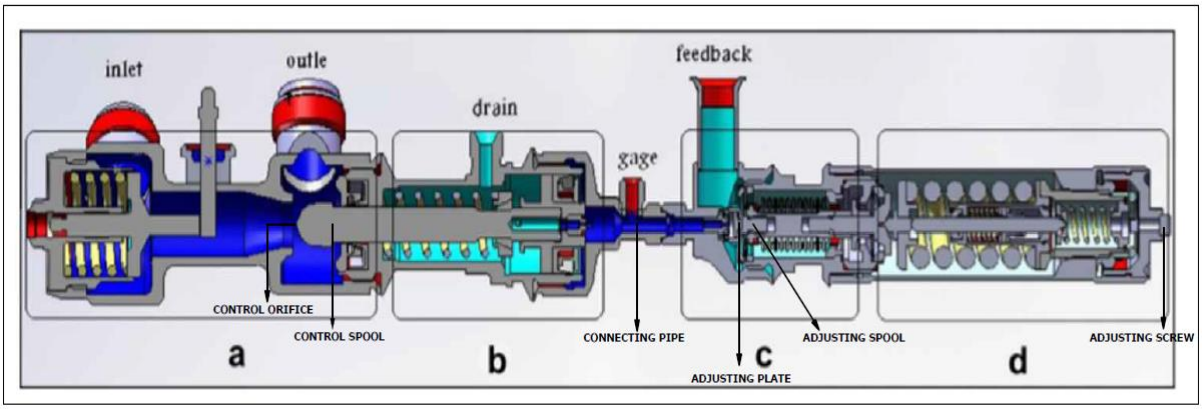

Figure 15: Proposed thrust regulator (pressure regulator)[1].

Working principle of the existing pressure control valve:

It should be mentioned that the proposed valve is designed so as to regulate its outlet pressure. The valve's working principle therefore has the goal of regulating the outlet pressure in the design state. From the following Fig. 16, it may be noticed that the entrance to the feedback pipe has been placed exactly on the outlet location (called the sense zone (6)). This valve's schematic reveals that, with the increase in inlet pressure, the pressure in both the feedback path and the adjusting part is increased. As

a result, this increased pressure the adjusting orifice to open (15). Thus, the pressure in the front zone (17) of the control piston (4) is increased, resulting in the control orifice closing (5). Eventually, with the decrease in the cross-section area of the passing flow, the entire pressure loss of the regulator is increased and thus the pressure increased in the outlet flow will be regulated. The valve's operational mechanism may initially seem to be straightforward; however major complications were experienced when modelling the system. The issues were associated with the interaction of simultaneous-dynamics between the fluid and the moving mechanical components of the valve[1].

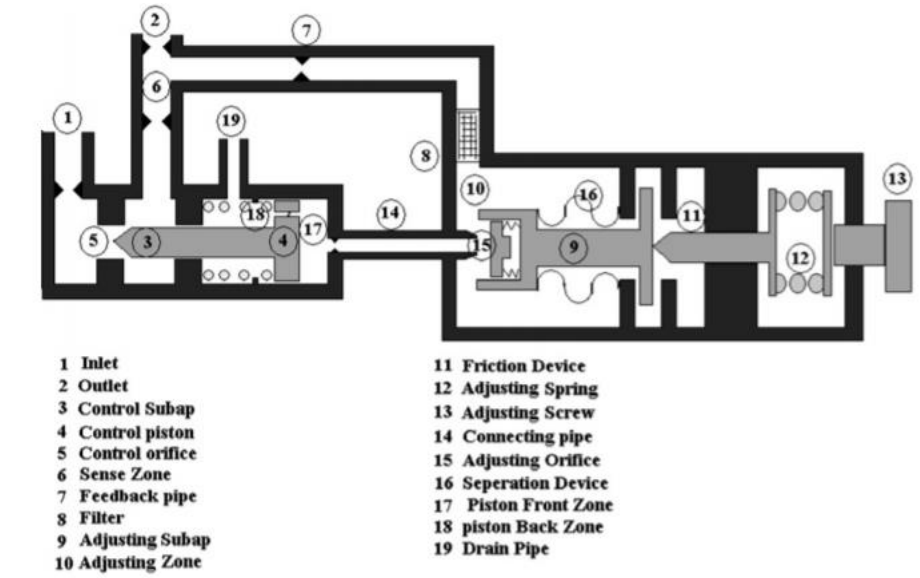

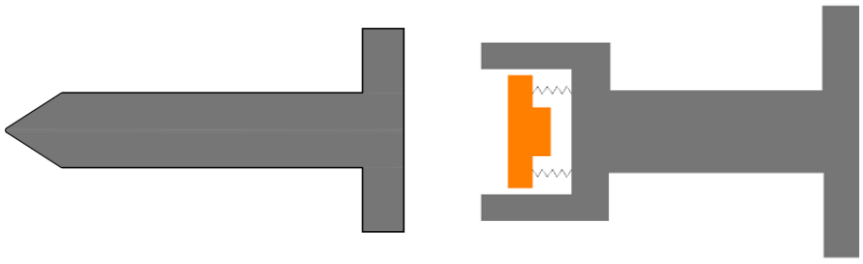

Control Spool **Adjusting spool with adjusting plate**
Orange body=adjusting pate

Figure 16: A schematic of the proposed indirect trust regulator (pressure regulator)[1].

4.3 Remodel the Adjusting Part of Pressure Control Valve:

In the original pressure control valve, which has been proposed by Dr. Amir, there are a total of three moving elements inside the system. They are the control spindle, adjusting spindle and adjusting plate or placoid. The analysis of the existing pressure control valve's dynamics reveals that during normal

operation, two of the moving elements, the adjusting spindle and the adjusting placoid, move together synchronously. This means that the relative positions of both the adjusting spindle and placoid remain the same throughout the valve's operation for various inlet pressures. Fig.17 shows the schematic for the position of both the adjusting plate (z) and adjusting spindle (y). The following Fig.18 represents the change in the adjusting spindle and plate's displacements. As it is represented in the graph, after each step, both the adjusting spindle and placoid remain in the upper area, producing a flat curve, meaning that the cross-section area of the adjusting orifice is widened. Thus, the pressure increases in the control section which causes the tip of the control spindle to move and remain in the high-pressure area. Therefore, to withstand the excessive force on the control spindle, a lower pressure drop is required in the adjusting section of the control valve.

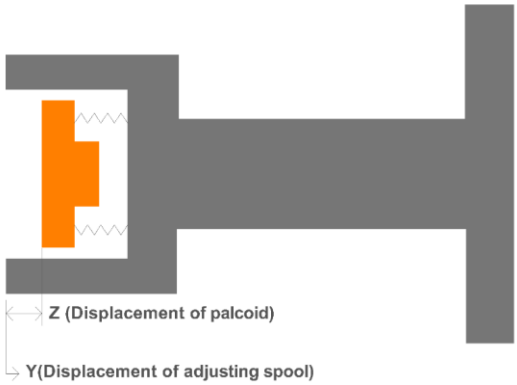

Figure 17: Schematic for the position of adjusting plate (placoid) (orange body) and spool (Grey body).

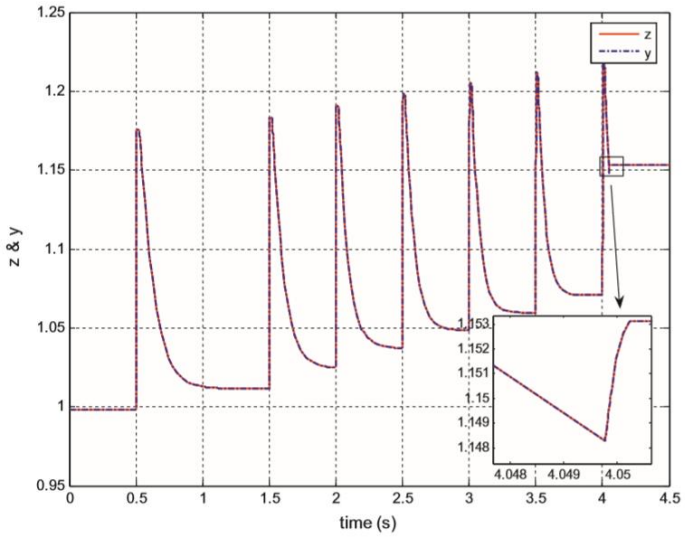

Figure 18: Graph of change in the adjusting spool (y) and adjusting plate (z)

Based on this behaviour, it is viable to consider the adjusting spool (spindle) and plate (placoid) together as one single adjusting spool (spindle) with no plate (placoid). This produces the following modified adjusting spool.

Figure19 : Adjusting spool (spindle) with plate or placoid (oragne body) in the left and modified adjusting spool in the right.

4.4 Develop Bond-graph model of the Remodelled-system

In order to investigate or analyse the dynamic behaviours of the proposed pressure control valve with the simplified adjusting part, a respective Bond-graph model has been developed. The Bond-graph model of the original control valve is attached below (Fig. 21) where bonds 57 and 60 represent the momentum and position of the adjusting placoid. I_{57}, and q_{60} denotes the placoid inertia and placoid spring capability. There are two placoid-resistances defined by R_{58} and R_{47}. For developing the Bond-graph model with a modified adjusting spindle, all the bonds that represent the adjusting placoid, along with the corresponding transformers (c, h, and I), have been eliminated, as the modified adjustment section has only a single moving element, that is, the adjusting spindle. To provide a clearer understanding, the schematic of the adjusting placoid with its Bond-graph elements is shown below in Fig.20.

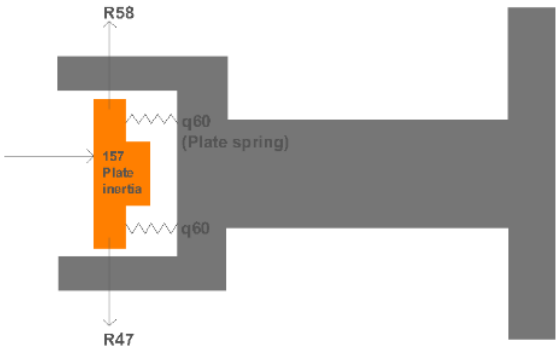

Figure 20: Schematic of adjusting placoid (Orange body) with its Bond-graph elements.

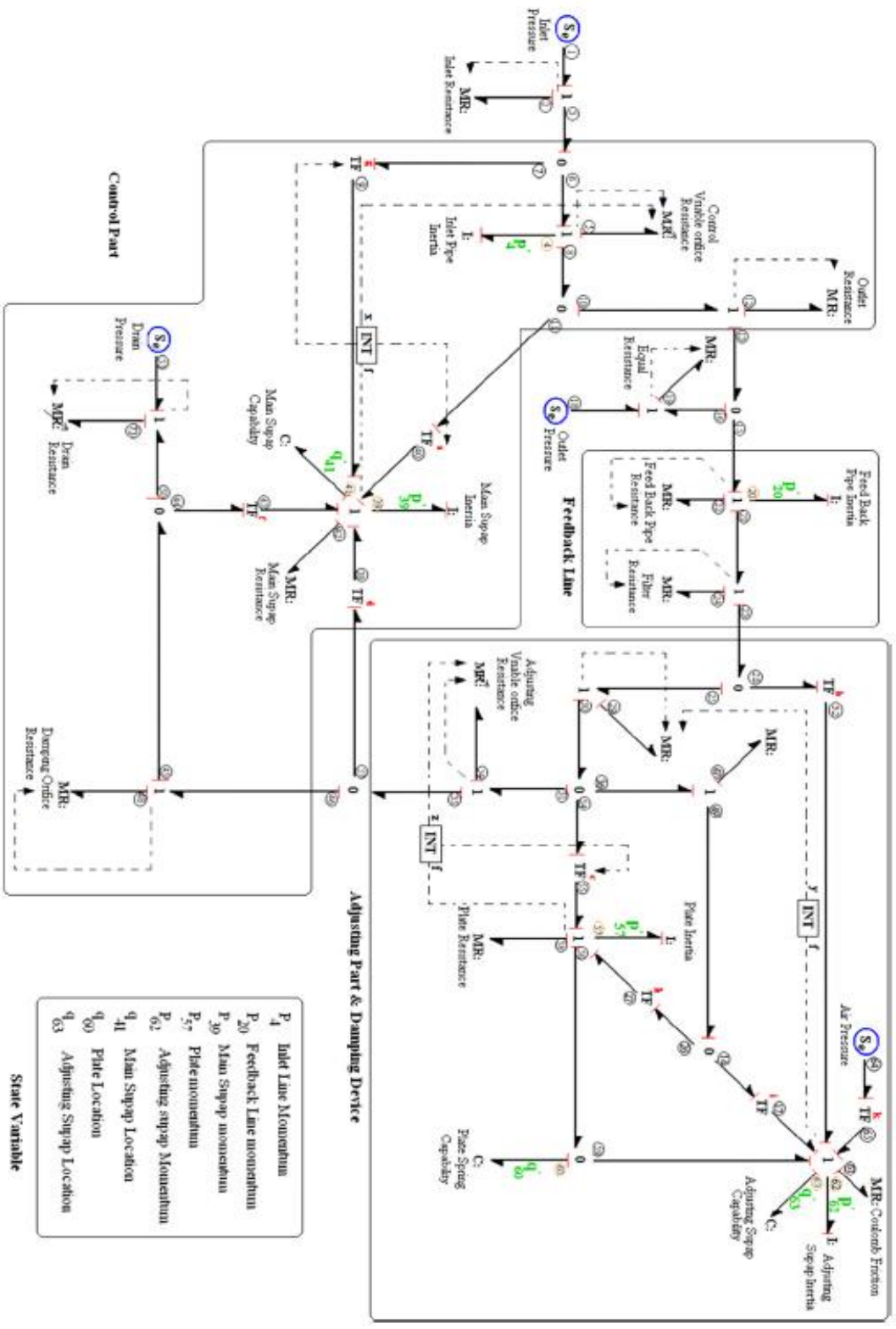

Figure 21: Bond-graph model of the original system[1].

Thus, the Bond-graph model of the modified control valve has been obtained, a diagram of which is shown below. After comparing the original and modified Bond-graph models, it is observed that the

original system is comparatively more complicated with eight state variables whereas the modified system has only six degrees of freedom (state variables). When developing the dynamic model of the modified system, the following assumptions were taken where[1]-

- Resistive and capacitive effects are lumped wherever required.
- Fluid inertia is considered.
- Capacitive characteristic for the diaphragms is considered.
- The outer pressure is considered as equal to the atmospheric pressure.
- A stable supply source is considered to control the inlet port.
- Mass of the diaphragm and spring is measured.
- For the analysis purpose, the fluid is considered to have the characteristics of an incompressible and Newtonian fluid.
- The stiffness coefficient of the spring is considered as a constant.
- The orifice's resistance is configured as a nonlinear function of the fluid flow rate.
- Temperature effect is considered as negligible.
- Every solid component is considered as rigid.
- Constant flow viscosity is assumed.

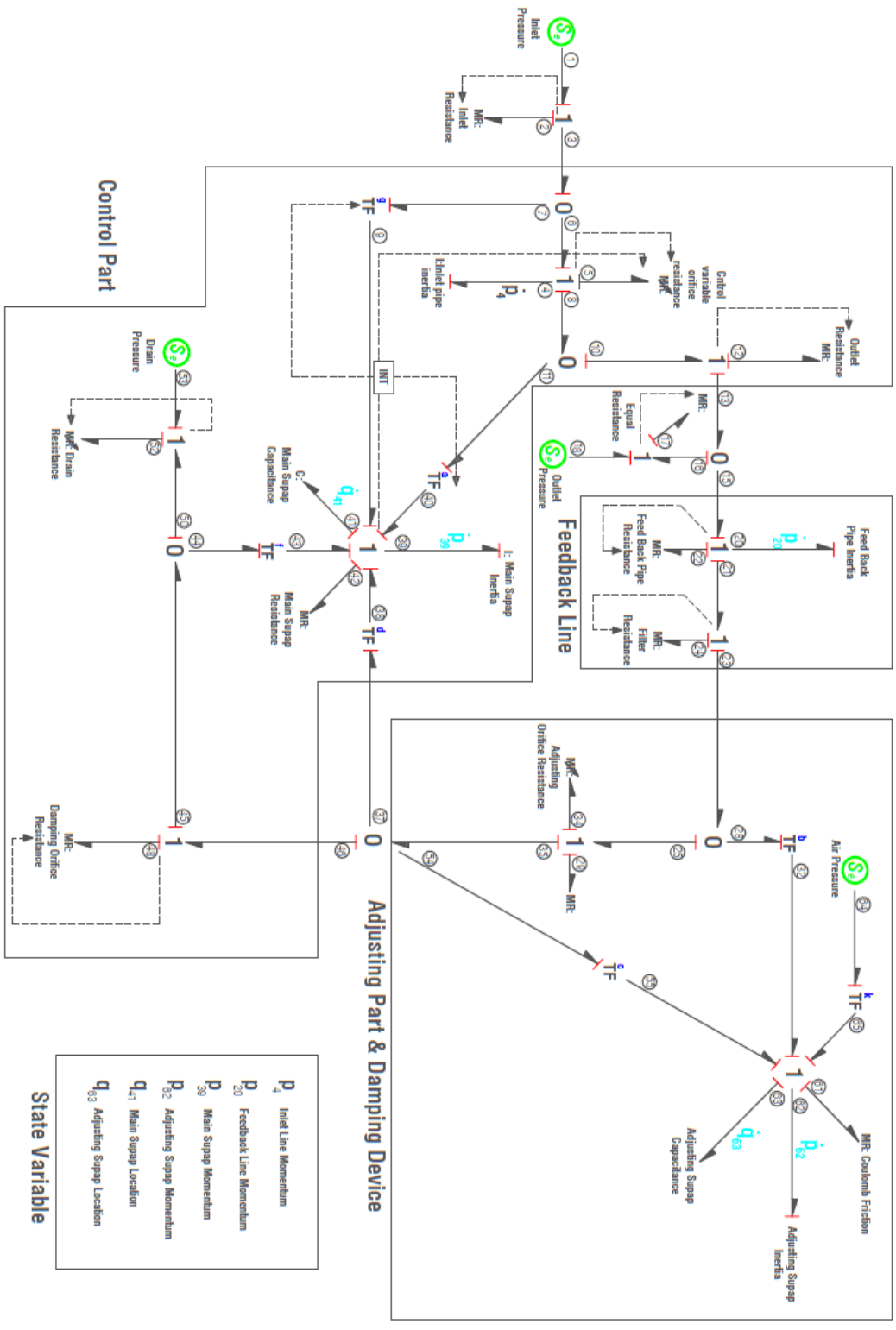

FIGURE:Bond Graph Model Of The Control Valve With Modified Adjusting Part

Figure 22: Bond-graph model of the modified system.

The newly developed Bond-graph model in Fig. 22 is able to display each different section (control section, feedback line & adjusting section) and main parameters of the pressure control valve clearly, as they are highlighted separately. In the Bond-graph model, the effort source element, Se1, denotes that the valve's inlet pressure has been supplied from a stable source to the control valve. Similarly, Se18, Se53, and Se64 elements represent valve's outlet pressure, drain pressure and air pressure respectively. All of them are stable sources of pressure and are considered to result from atmospheric pressure (P_{atm}). This modified pressure control valve has two moving mass elements: the control spindle or spool and the adjusting spindle on which the majority of system's dynamic properties depend. In the Bond-graph, bonds 39 and 41 reflect the control spool momentum and position respectively. For the adjusting spool, bonds 62 and 63 do the same. The damping device of this pressure control valve has a direct effect on the adjusting spool which is simulated with a coulomb damper. Bond 61 represents this coulomb friction in the presented Bond-graph.

4.5 Extracting Mathematical Equations from the Developed Bond-graph Model

In this stage, the state space differential equations for all six state variables as mentioned in the Bond-graph of Fig. 22 have been derived by applying rules for extracting mathematical equations from respective Bond-graph model. Using the similar procedure that has been mentioned in chapter 3, the mathematical equations for all these six state variables have been extracted manually.

Obtained state variables equations from the simplified Bond-graph model:

$$\dot{p}4 = e4 = -\left(-\frac{ap39}{I39}+\frac{p4}{I4}\right)R12-\left(-\frac{p20}{I20}-\frac{ap39}{I39}+\frac{p4}{I4}\right)R19-\left(\frac{gp39}{I39}+\frac{p4}{I4}\right)R2-\frac{p4R5}{I4}+Se1+Se18 \quad (1)$$

$$\dot{p}20 = e20 = (-\frac{p20}{I20}-\frac{ap39}{I39}+\frac{p4}{I4})R19-\frac{p20R22}{I20}-\frac{p20R24}{I20}-(\frac{p20}{I20}-\frac{bp62}{I62})R29-(\frac{p20}{I20}-\frac{bp62}{I62})R34-(\frac{p20}{I20}-\frac{dp39}{I39}-\frac{bp62}{I62}-\frac{cp62}{I62})R48-(\frac{p20}{I20}-\frac{dp39}{I39}-\frac{fp39}{I39}-\frac{bp62}{I62}-\frac{cp62}{I62})R52-Se18+Se53 \quad (2)$$

$$\dot{p}62 = e62 = -\frac{q63}{C63}+c((\frac{p20}{I20}-\frac{dp39}{I39}-\frac{bp62}{I62}-\frac{cp62}{I62})R48+(\frac{p20}{I20}-\frac{dp39}{I39}-\frac{fp39}{I39}-\frac{bp62}{I62}-\frac{cp62}{I62})R52-Se53)+b((\frac{p20}{I20}-\frac{bp62}{I62})R29+(\frac{p20}{I20}-\frac{bp62}{I62})R34+(\frac{p20}{I20}-\frac{dp39}{I39}-\frac{bp62}{I62}-\frac{cp62}{I62})R48+(\frac{p20}{I20}-\frac{dp39}{I39}-\frac{fp39}{I39}-\frac{bp62}{I62}-\frac{cp62}{I62})R52-Se53) \quad (3)$$

$$\dot{p}39 = e39 =$$

$$-\frac{q41}{C41}-\frac{p39R42}{I39}+g(-(\frac{gp39}{I39}+\frac{p4}{I4})R2+Se1)+a((-\frac{ap39}{I39}+\frac{p4}{I4})R12+(-\frac{p20}{I20}-\frac{ap39}{I39}+\frac{p4}{I4})R19-Se18)+f((\frac{p20}{I20}-\frac{dp39}{I39}-\frac{fp39}{I39}-\frac{bp62}{I62}-\frac{cp62}{I62})R52-Se53)+d((\frac{p20}{I20}-\frac{dp39}{I39}-\frac{bp62}{I62}-\frac{cp62}{I62})R48+(\frac{p20}{I20}-\frac{dp39}{I39}-\frac{fp39}{I39}-\frac{bp62}{I62}-\frac{cp62}{I62})R52-Se53) \quad (4)$$

$$\dot{q}41 = \quad p39/I39 \quad (5)$$

$$\dot{q}63 = \quad p62/I62 \quad (6)$$

In addition to this set of six state variables, there are 92 auxiliary equations that configure all the essential parameters of the developed Bond-graph model of the proposed system. The most fundamental parameters are the inertia coefficient (I_i), capacity coefficient (C_i), resistant element (R_i), and pressure transformer (TF_i). As some of the parameters are time variant, the system has nonlinear dynamics. The parameter I_i represents the inertia coefficient of ith element and a similar pattern is followed for the rest of the parameters. There are two different types of sub-systems that form the system of concern, namely the mechanical sub-system and the hydraulic sub-system. In every sensitive control valve, such as the pressure control valve, there are narrow feedback pipes. It is therefore important to study the hydraulic inertia impacts on the system when the fluid dynamic is being considered. According to the laws of physics, energy consumption is required when changing the fluid velocity and thus an induced acceleration to the fluid stream causes changes in the pressure of the feedback pipe ($\dot{p}20$). In addition, the respond time to the outlet distributions must be reduced in the pressure control valve – however the inertia parameter of the system opposes this condition. It is essential that this issue be considered while modelling the system. Both the inlet (I_4)and feedback pipe (I_{20})inertia coefficients are very significant parameters of the system. According to the Newton's law, the formula for determining the linear inertia coefficient is [17]-

$I_i = \rho\sum\frac{L_j}{A_j}$, where L= length and A= area

The inertia coefficient of a mechanical system may be defined as the mass of a moving body, including the fluid mass. There are two moving elements in the modified system. Therefore, the inertia factors presented in the developed Bond-graph are I_{39} and I_{62}, defining the moving elements of the control and adjusting sections respectively.

In the resulting mathematical equations, the resistant coefficient of Bond-graph's i^{th} element of the Bond-graph model is represented by R_i. In the proposed hydro-mechanical system, most of the resistant elements are defined as a hydraulic type. All resistant elements in the pressure control valve are shown in Fig. 23.

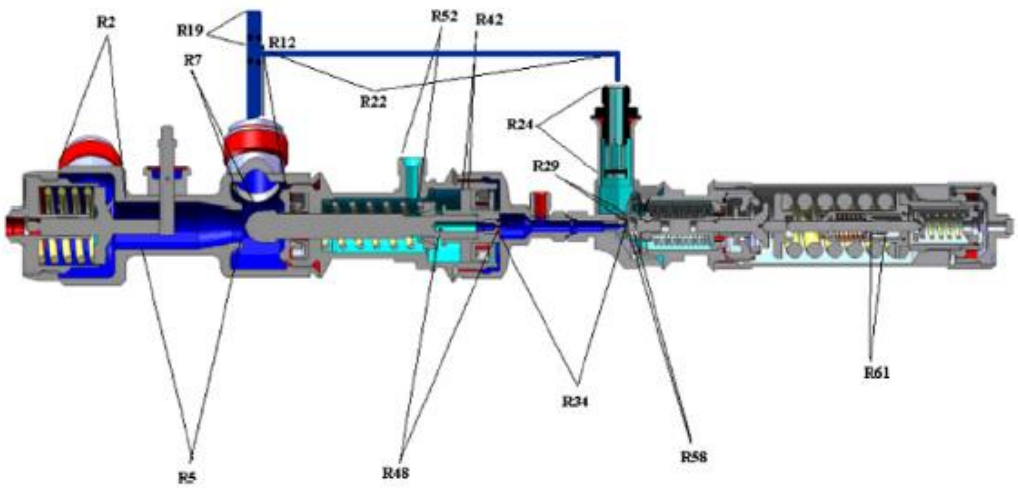

Figure 23: Arrangement of resistant elements in the pressure control valve.

In the developed Bond-graph model, the resistant element's coefficients has been formulated as [17]-

$R_i(\rho, \dot{Q}, \xi) = \rho|\dot{Q}|\xi_i$, where ρ is the density, $Q$is the volumetric flow (for the hydraulic system) and ξ denotes pressure loss in general. The formula used for determining different pressure losses is determined to be:

$$\xi_i = \left(\frac{\sum\zeta_l}{2A_{l\,min}^2} + \frac{\zeta_f}{2A_{f\,min}^2}\right)_i$$

In the above formula, ζ_l and ζ_f define the respective local and friction pressure loss. From Fig. 23, the resistant elements denoted by R_2 , R_5 , R_{12} , R_{19} , R_{24} , and R_{48} are the set of local pressure losses which are constrained by the valve's geometry. This set of local pressures is associated with the following resistant coefficients:

R_2 = inlet resistant coefficient

R_5 = Control orifice variable resistant coefficient

R_{12} = outlet resistant coefficient

R_{19} = Equal resistant coefficient

R_{24} = Feedback line resistant coefficient

R_{48} = Damping orifice resistant coefficient

R_{22} is also associated with the feedback pipe resistant which may be calculated with the consideration to the diameter and length of the feedback pipe, via the following formulae:

$$\zeta_f = \lambda \frac{l_{feed}}{D_{feed}} \qquad (7)$$

$$\lambda = 0.11\left(\bar{h} + \frac{68}{Re}\right)^{0.25} \quad (8)$$

$$Re = \frac{1.12838Q_{feed}}{\upsilon A_{feed}^{0.5}} \quad (9)$$

The most significant resistant elements of the proposed valve are associated with the control (R_5) and adjusting (R_{34}) orifices. Fig. 24 shows the direction of motion of control spool, denoted by the x direction. Movement following the x direction of the control spool results in significant changes to the control orifice's cross-section area. According to the Fig. 24, the aerodynamic geometry of the control spool head reveals that the shape of the peripheral surface is a truncated cone, causing the flow to bend over the surface on the smooth profile.

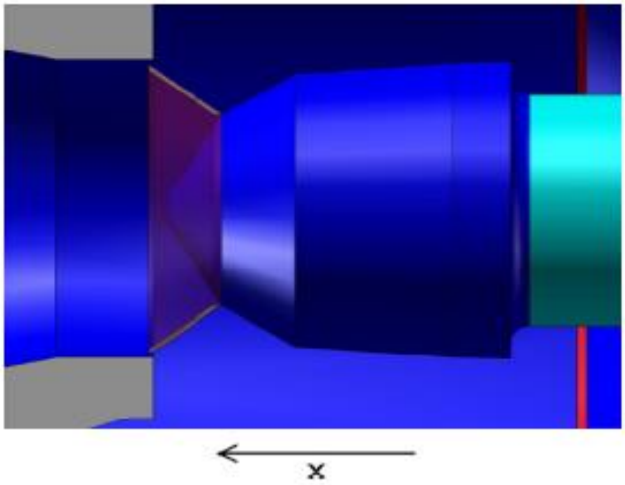

Figure 24: Direction of motion of control spool

The formulation for the coefficient of the resistant element in the Bond-graph is shown below.

$$R_5 = \frac{\zeta_{Regulator}}{2A_{hms}^2}\ \rho\left|\dot{Q_{in}}\right| \quad (10)$$

$$\zeta_{Regulator} = \frac{A_{hms}}{Re_h} + \left(1 - \frac{A_{hms}}{A_{in}}\right)^2 + 0.18 \quad (11)$$

$$A_{hms} = \frac{\pi}{sin\alpha_i}\left(R_0^2 - \frac{1}{4}X_h^2 sin^2 2\alpha_i\right) \quad (12)$$

$$X_h = X_i' + x \quad (13)$$

The resistant element of the adjusting orifice, R_{34}, is another significant resistant coefficient by which the cross-section area may be varied, with the displacement of the adjusting spool in the y direction.

This is shown in the Fig. 25. Using the following formula, the adjusting orifice resistant coefficient can be determined.

$$R_{34} = \frac{\zeta_{loc.adjust}}{2A_{Ado}^2}\rho\left|\dot{Q}_{feedback}\right| \quad (14)$$

Here, $\zeta_{loc.adjust}$ = the local pressure loss in adjusting orifice,

$Q_{feedback}$ = the feedback pipe volumetric flow

And, A_{Ado} = the area of adjusting orifice depends on the diameter of the area and length in terms of the displacement of the adjusting spool (y).

Moreover, there are an additional two important resistant elements in the developed Bond-graph model, namely R_{42} and R_{61} ,that affect the two moving elements of the control valve. These resistant elements oppose the corresponding control spool and adjusting spool through coulomb friction.

Another major Bond-graph element is the capacity coefficient. The two most significant capacity coefficients for the proposed system are C_{41} and C_{63} representing the capacity factor for the respective amplifying or control section and the adjusting section. As per the formula, these capacity coefficients can be configured as inversely proportional to the spring's stiffness, as shown below:

$$C_{41} = \frac{1}{k_{controlSp.}} \quad (15)$$

$$C_{63} = \frac{1}{k_{eq.Adj.}} \quad (16)$$

Here, $k_{controlSp.}$ = the spring stiffness of control section and

$k_{eq.Adj.}$ = the equal spring stiffness of the adjusting section.

As emphasised earlier, one of the most substantial advantages of using the Bond-graph approach is its ability to model different sub-systems with different energy domains, via its eponymous procedure. Therefore, to allow this energy-conversion from one sub-domain to another, the Bond-graph model is required to transform its elements. These elements allow the transformation of the kinematic energy among hydraulic and mechanical (mass-spring) subsystems in every time instance. Therefore, pressure transformers which consist of a solid spool or piston moving under fluid pressure from two different levels, must be considered while modelling. There is a total of seven pressure transformers in the concerning system, namely $a, b, c, d, f, g,$ and k .

Transformers a and g are associated with the surface of the control spool head which refers to the surface area both before and after the control orifice, as shown in Fig. 25. From the figure, it may be

anticipated that calculating the hydrodynamic force acting on the control spool tip or head will be extremely complicated while the fluid flow is passing the control spool tip's surface.

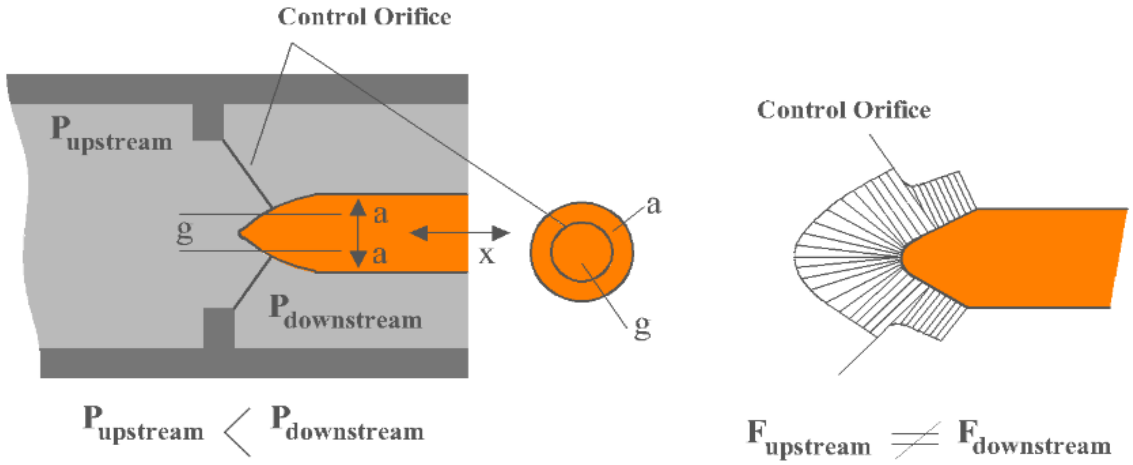

Figure 25: Pressure distribution schematic on the surface of control spool head.

Additionally, changes in fluid velocity occur due to the shape of the control orifice when passing through the surface. Thus, changes in fluid velocity result in a variable pressure distribution on the control spool by contracting the fluid flow. The changes in pressure profile is therefore required to establish the force balances on the control spool since the fluid flow is passing over the control orifice. These transformer elements a and g can be configured by the following equations when the motion of the control spool is regarded.

$$a = \frac{\pi}{4}\left(D_{tms}^2 - X_h^2 sin^2 2\alpha_i\right) \tag{17}$$

$$g = \frac{\pi}{4}\left(X_h^2 sin^2 2\alpha_i\right) \tag{18}$$

There are two other transformer elements relate to control spool which are d and f.These transformer elements are associated with the front and back zones of the control spool respectively. In the Bond-graph model, the transformer elements for adjusting part namely b and c allow the conversion of hydraulic energy to mechanical via the adjusting spool.

4.6 Simulation of System Dynamics:

To perform the simulation of the control valve's dynamic behaviours, some of the required physical constraints have been introduced to the software through different sub-programs. These physical constraints include the domain of each element's motion, and their frictions or collisions, programmed by utilising the spindles' measurements of forces and velocities along with their directions. These respective sub-programs were written with consideration to the position of the two moving elements at

every time step. A reset signal was transmitted to the integrator side in order to build them into a level situation, so that the main program could figure out exactly when and where those collisions have occurred. Moreover, inside these sub-programs, allowances for coulomb friction was inserted to the equations. The final step towards the completion of the simulation involved solving the set of equations by using the ODE15s solver. This kind of variable order solver requires numerical differentiation formulas.

The resulting simulation results may be verified by comparing them against a benchmark, which is the result from the existing original system (pressure control valve).

4.7 Simulation Results and Analysis:

In this step, the obtained simulation results for different operations, considering different parameters of the modified system, have been illustrated and compared with the original system's simulation results. Additionally, an analysis of the simulation results achieved from the modified system is presented. It must be mentioned that the presented results are dimensionless.

As the proposed system is a pressure regulator, as shown in Fig. 25 the pressure regulation in the control part of the modified system is compared with that of original system. The graph of Fig. 26 reveals that, with the step input, at time equals to 1 second the pressure is regulated. In the modified system, the quick drop of pressure demonstrates that pressure regulation in the modified system is significantly faster than in the original system. In the original system, at time = 1.5sec, the change in pressure has dropped to the operational value whereas in the modified system, it took around 1.1sec.

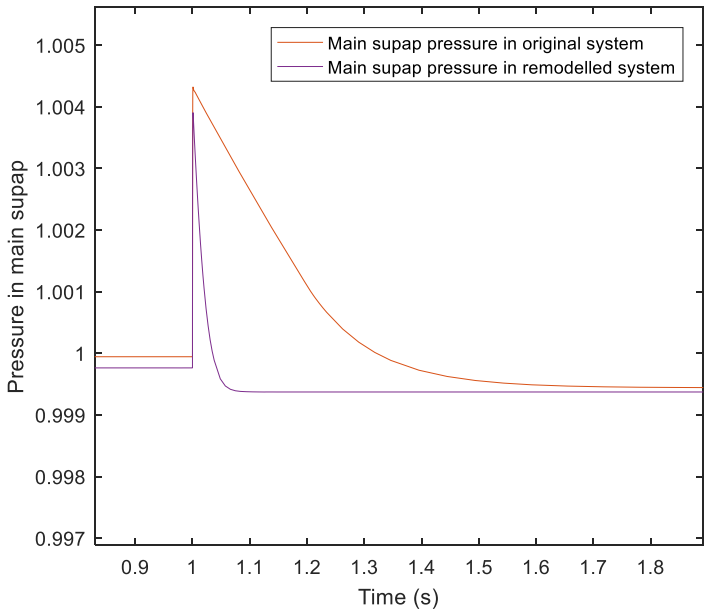

Figure 26: Graph of the comparison of pressure in main-supap (control part) between the original system and modified system.

As mentioned earlier, the proposed pressure control valve performs regulation by changing the cross-section area of both the control and adjusting orifice. This cross-section area depends on the displacement of the valve's two moving components, namely the control spool and the adjusting spool. Therefore, for the control valve to work with appropriate operational settings, it is very important to compare the displacement of the spools of modified system with that of the original system. Fig. 27 illustrates the displacement of the control spool in both the modified system and the original system. As it is shown, the increase in inlet pressure results in an increase in the pressure of the amplifying section, indicating a pressure rise in the front zone of the control spool (piston). Thus, the control spool moves resulting in a narrow control orifice which decreases the pressure flow from the inlet. The displacement of control spool is faster and more sudden in the modified system in comparison to the original system, demonstrating that the control spool's collision with the amplifying section's wall happens faster in the modified system. It also indicates that in the modified system, the signal for incremented pressure transmits through the feedback pipe with a shorter delay than that of the original system. Thus, the displacement occurs at the moment of increase in pressure. This collision happens because of the system's hydraulic properties, and because of the existing inertia of the mechanical element. Therefore, the mechanical inertia is one of the most vital parameters for maintaining accuracy of the system. Moreover, coulomb friction has been considered while simulating this dynamic.

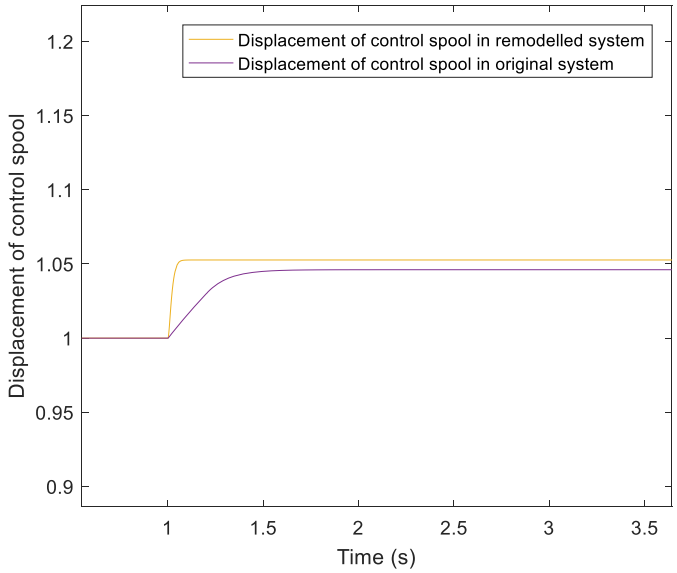

Figure 27: Comparison of the displacement of the control spool between modified system and original system.

The graph of the adjusting spool's displacement in both the modified and original systems is shown in Fig. 28. It may be observed that in modified system the displacement is significantly faster and higher

than that of original system, demonstrating that the modified system's higher displacement causes a larger opening of the adjusting orifice. Thus, the pressure in control section of the control valve rises more quickly. The curve of displacement in original system reveals that the adjusting spool reaches the upper region and remains there for a while, as shown by the flat curve from 1s to 1.2s. This is explained by the presence of coulomb friction in the adjusting section. This flat line defines the adjusting spool's required time to overcome the friction and move to its original location. In the modified system, the sharp peak illustrates that the level of coulomb friction is much lower.

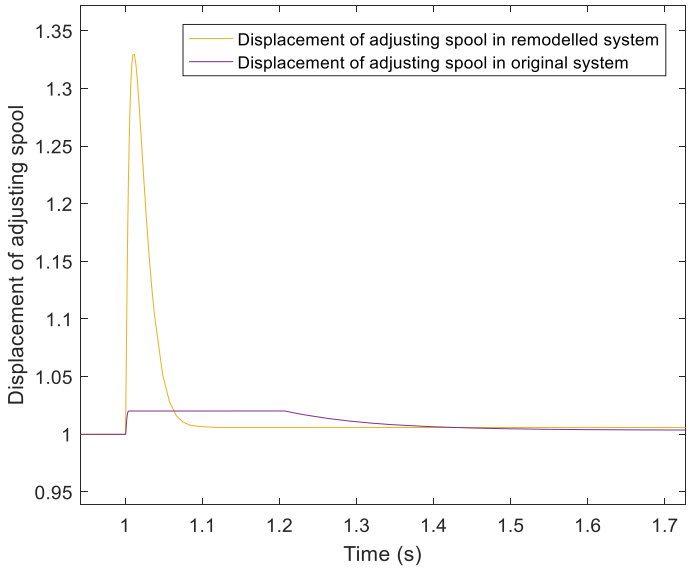

Figure 28: Comparison of the displacement of the adjusting spool between modified system and original system.

Based on the above-mentioned critical analysis of Fig. 26 to 28, it can be concluded that, like the original system, the modified system regulates the pressure by following the same principle of changing the moving element's orifice cross-section area, but in a shorter length of time. The modified system with fewer moving elements is more effective and faster than the original system.

In a hydromechanical system, the analysis of variations in flow is required. Fig. 29 illustrates the graph of two most significant flows of the control valve, namely inlet flow and feedback pipe flow. As shown, the variation in the flow of feedback pipe is greater than in the inlet path or main path, with regard to the physical aspect of the system. Due to the mechanical inertia, when there is an increase in the entrance pressure of the feedback line, the adjusting section's condition remains same, just in the initial step. With the increase in pressure an instant rise in flow rise is occurred.

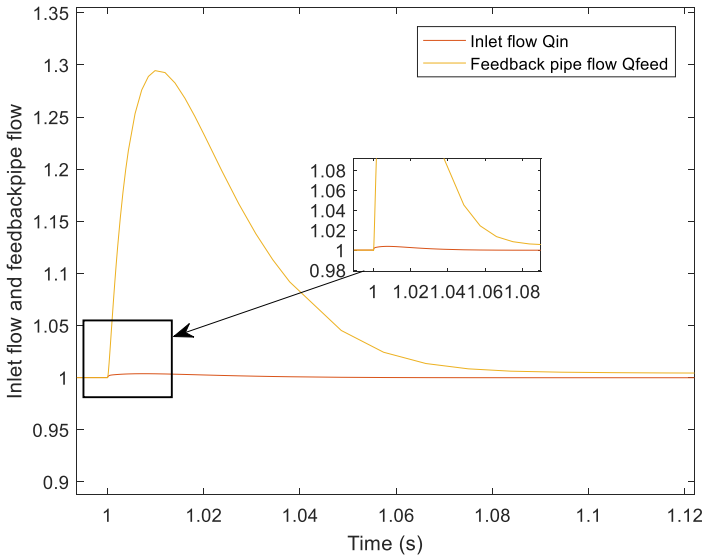

Figure 29: The graph representing the change in flow of inlet and feedback pipe

In this chapter, a nonlinear model of the pressure control valve has been obtained by means of the Bond-graph approach, in which significant modifications have been done to the valve's most sensitive part, the adjusting section. The resultant physical model of the proposed valve reflects the capability of the domain independent Bond-graph approach in modelling such nonlinear physical systems. The accuracy of the obtained model has been confirmed through simulation benchmarking, in which the most significant dynamics of the modified system were compared with the respective dynamics of the original system. This benchmarking proves that the modified system controls pressure using the same principles as original system, but even more effectively. While modelling, several nonlinearities were considered, as in original system. Additionally, the impacts of all significant parameters were considered, and as a result the modified system can be said to accurately represent the physical behaviour of the valve during operation.

5 Chapter 5: Modification of the Existing Model of Pressure Control Valve for Thermal Investigation

According to a study of Fangpo and Amir where they have proposed the elasto-expansive model of the spools, the thermomechanical phenomena of the system can be addressed by incorporating this elasto-expansive model of the spools into the newly developed Bond-graph model of the pressure control valve with modified adjusting part[18]. The proposed thermos-elastic model of the spool is capable of investigating the coupled effects of structural expansion and softening of materials inside the spool by offering the desired physical meanings into the system dynamics. In this chapter, the pure elastic spool has been modelled by means of Bond-graph approach and the dynamics of elasticity has been analysed which confirms the elastic spool's capability of being flexible.

5.1 Bond-Graph (BG) Modelling of the Elastic Spool:

The geometry of the both spools in the hydro control device reveals that it is possible to consider each segment of the spool as beam members. These beam members can be treated as having their own distributed parameter systems directed by the partial differential equations, but for finite approximation may be lumped into space [8]. The proposed discretely lumped structure of the spool is appropriate for developing the thermos-elastic model of the spool. Though the internal interface between the elastic and thermal subdomains of the spools are certainly distributed, the complete configurations of both spools can be individually designed by the lumped elements. Such obtained models of the spools possess not only the numerical characteristics but also the analytical characteristics, while representing the internal multi-physical behaviours of the system. According to the nature of the BG approach, this can represent both the distributed parameter and lumped systems seamlessly. Therefore, the BG approach has been chosen as a modelling tool for the beam configuration of the spools. The BG technique of modelling does not apply any approximations to the lumping process and is able to present a complete discrete-numerical configuration of the spools in an efficient way[8].

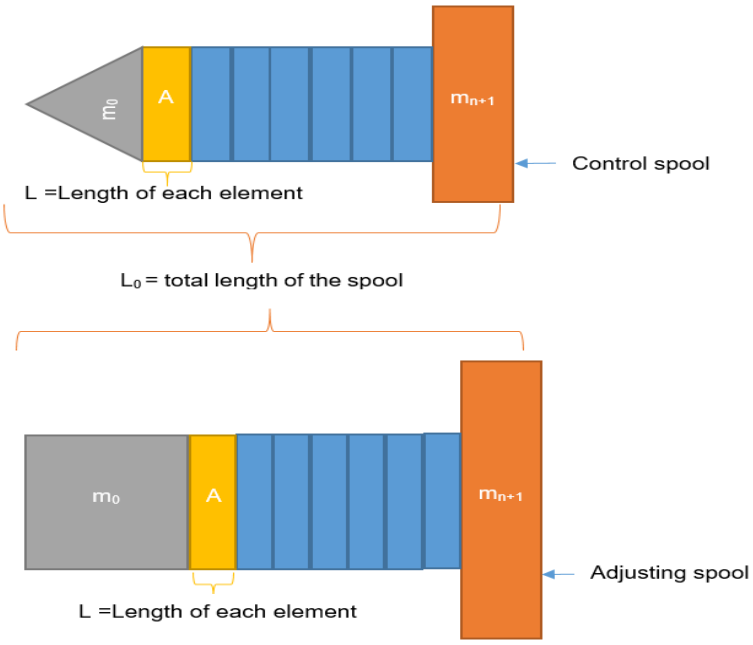

Figure 30: Schematic of Elastic control &adjusting spool.

Fig. 5 reveals the actual shape of both spools. The grey and orange shaded portions are denoted as the front and back, with different shapes respectively, and the middle part is a uniform beam in a rectangular shape that can be assumed to consist of large number of elements. The yellow shaded area represents one element where the length and area of each element is denoted with L and A. The masses (m) of each element are also considered to be equal. As the shape of the spool is circular, the area of a circle in terms of diameter is the associated area for each element of the spool.

A = $\frac{\pi D^2}{4}$, D is the diameter of the circle.

L_0 = the total length of the spool.

Thus, if the total no. of element is n, the length of each element is, $L = \frac{L_0}{n}$. A simple beam structure of three elements has been shown in Fig. 31 which represents the configuration of each element.

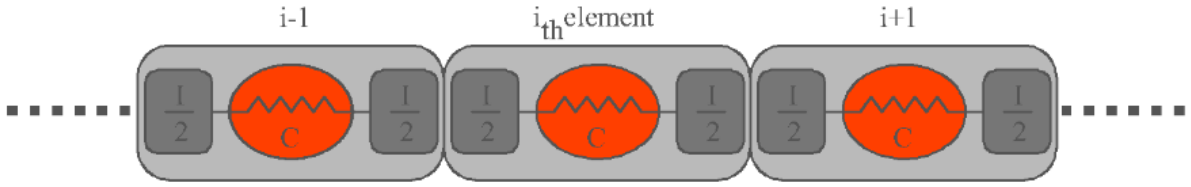

Figure 31: A simple beam structure with three elements.

The above figure illustrates that each element has two different storage components, inertia and capacitance. As it has been already mentioned in chapter 3 that inertia stores kinetic energy and capacitance stores potential energy. In each element of beam structure, the inertia component (I) has been distributed to both sides at the boundary of the element, and the capacitor component (C) has been placed at the centre. Therefore, the potential energy will be stored at the centre of the reticulated space and the kinetic energy will be stored at the boundary of both sides of each element. As the above-mentioned configuration of reticulated beam structure is continuous, boundaries of any two adjacent elements will move jointly. Therefore, this configuration can be used as a junction-element chain where the parameters of this junction can be formulated by the associated parameters of two adjacent elements. The respective Bond-graph model of the above-mention beam structure with three elements is shown in Fig. 32.

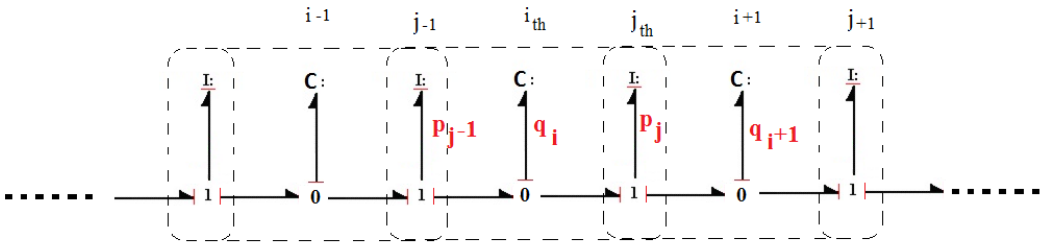

Figure 32: Bond-graph model of the elastic beam structure.

In the Bond-graph model of the elastic beam structure, there are two different state variables for i_{th}element and j_{th} junction which are q_i and p_j. q_i represents the deformation of the i_{th} element and p_j represents the momentum of the j_{th} element. The state equation for each element has been derived as per conservation of energy from the Bond-graph model.

$$\dot{q}_i = \frac{p_{j-1}}{I_{j-1}} - \frac{p_j}{I_j} \tag{19}$$

$$\dot{p}_j = \frac{q_i}{C_i} - \frac{q_{i+1}}{C_{i+1}} \tag{20}$$

$$I_j = \frac{m_i}{2} - \frac{m_{i+1}}{2} \tag{21}$$

Here I_i is the boundary inertia which has been considered as a function of masses$(m_i \; and \; m_{i+1})$ of two adjacent elements. As the mass of each element is constant, the inertia component has been considered as a constant here. The capacitance component has also been considered as a constant which is a function of geometry and parameters related to the i_{th}

element. To derive the capacitance component, in this 1-D Hook's strain stress expression has been used which is:

$$\sigma = E\mathcal{E} \tag{22}$$

Where σ, E, and $\mathcal{E}$ are the axial stress, strain and elasticity modulus respectively. For a simple beam structure of axial spool, Hook's law can be rewritten for each junction considering the capacitance for each junction is equal and constant. Hook's law for simple axial spool is:

$$F = \frac{AE}{L} q \tag{23}$$

Where F has been considered as the applied collective force to the junction and q is the deformation of each element. A is the area of each element and L is the length of each element of the spool which is equals to $\frac{L_0}{n}$ for n number of element.

Now, $\dot{p}$ is the pressure (in hydraulic system) or force (in mechanical system) which in terms of deformation and capacitance can be written as:

$$\dot{p} = \frac{q}{C} \tag{24}$$

Besides, when $\dot{p}$ is mechanical force it can be written as:

$$\dot{p} = m\ddot{x} \tag{25}$$

Where m is the mass and $\ddot{x}$ is the acceleration. So, according to Newton's law:

$$F = m\ddot{x} \tag{26}$$

From equations 18, 19 and 20 it can be derived that:

$$F = \frac{q}{C} = \dot{p} \tag{27}$$

Considering equation 17 and 21, the capacitance factor can be written as:

$$C = \frac{L}{AE} \text{ or } C = \frac{L_0}{AEn} \tag{28}$$

According to the valve's geometry, the first and last element of the elastic spool which are indeed the left-end and right-end element, will receive external mechanical forces to the beam structure. Therefore, the state variable equation for the first and last element will be in terms of those external mechanical forces. Equation (14) can be re-written accordingly:

$$\dot{p}_J = F_l - \frac{q_{i+1}}{C_{i+1}} \tag{29}$$

$$\dot{p_J} = \frac{q_i}{C_i} - F_r \quad (30)$$

Here, F_l and F_r are the left and right end mechanical loadings or forces acting on the first and last element of the elastic spool respectively. Thus, applying equations (13), (14) and (15), a distributed Physical elastic model of the spool has been formed which is able to describes the true physical dynamics of being pure elastic in nature. The resultant elastic model of the spool possesses the feature of these mathematically derived governing equations along with the feature of numerically distributed beam structure's elements. Thus, this elastic spool becomes capable of providing a platform in which the desirable multi-physical dynamics has been simulated with respect to the alternation of associated parameters.

5.2 Modifying the Bond-graph Model of the System with Elastic Adjusting spool:

In this step, the resultant elastic spool has been incorporated into the existing Bond-graph model of the modified pressure control valve. As there are two moving elements in the valve, control spool and adjusting spool, at first the adjusting spool (rigid) has been replaced with the elastic adjusting spool. According to the Bond-graph model of the modified control valve, bond 62 and 63 represents the momentum and position of adjusting spool. As the rigid adjusting spool has been replaced with the elastic one, the bond 62 is now no longer a single junction, representing single state variable. The number of junction and state variable depends on the number of elements of the elastic spool. For n number of element, Fig. 33 represents chain of bonds associated with state variables from $\dot{p_{62}}_{(1)}$ to $\dot{p_{62}}_{(n)}$ which defines the momentum of 1st element to momentum of nth element (last element) respectively. Similarly, there is a set of state variables for the position or deformation of each element denoted by $\dot{q}_{(i)}$ to $\dot{q}_{(n)}$ where i equals to the number of element of n.

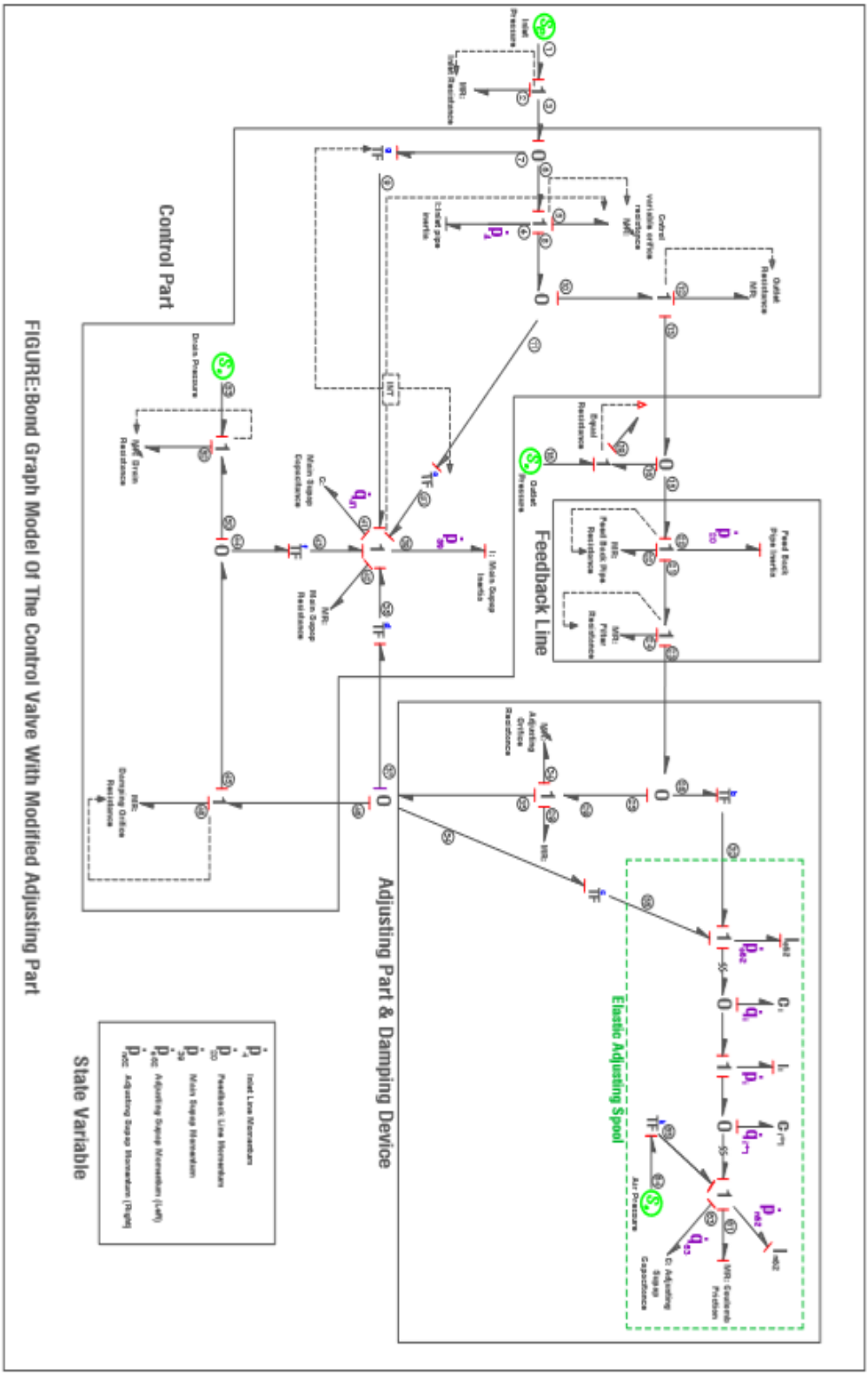

Figure 33: Bond-graph model of the modified pressure control valve with elastic adjusting spool.

5.3 Extracting Mathematical Equations (State Equations) of the Modified System with Elastic Adjusting spool:

As the rigid adjusting spool has been replaced with the elastic one, the above obtained Bond-graph with elastic spool will provide new set of equations of all those state variables that have been achieved in chapter 4. The state variable associated with the elastic adjusting spool, $\dot{P_{62}}$ has been extracted from the above Bond-graph with the help of equation (13), (14), (15), (23), and (24). According to the Bond-graph in Fig. 33, the mechanical force acting on the very left end element of the elastic adjusting spool comes from the two transformers b and c. As it has been mentioned previously that these two transformers convert hydraulic energy to mechanical in the adjusting part. The left and right end mechanical forces F_l and F_r have been represented by pdot62_fl and pdot62_fr in the set of equations. At this stage, a separate piece of MATLAB code has been written which has been added to the main body of the MATLAB code as a sub-program for elastic spool. This piece of code for elastic spool has been programmed in such a way where the number of elements can be varied by putting different values of n to achieve desired flexible spool. As the more the number of elements is, the more flexible the spool is. The following Fig. 34 shows the calculation for the state variables of elastic adjusting spool associated to both the momentum and position of each element.

Calculation of q_dot62:

$q\_dot62 \;=\; size(n);$

$q\_dot62(\,1) \;=\; 2 * p62(1)/I \;-\; p62(2)/I;$
$q\_dot62(\,n) \;=\; p62(n)/I \;-\; 2 * p62(n+1)/I;$

$for\ i = 2:(n-1)$
  $q\_dot62(\,i) \;=\; p62(i)/I \;-\; p62(i+1)/I\;;$

Calculation of p_dot62 :

$p\_dot62 \;=\; size(n+1);$
$p\_dot62(\,1\,) \;=\; pdot62\_fl - q62(1)/C\;;$

$for\ i = 2:n$
  $p\_dot62(\,i\,) \;=\; q62(i-1)\,/\,C \;-\; q62(i)/C\;\;;$

$p\_dot62(\,n+1\,) \;=\; q62(n)/C + pdot62\_fr\;;$

Figure 34: Equations (from MATLAB code) for determining state variables of elastic adjusting spool.

In the above-mentioned equations (MATLAB code), p_dot62 and q_dot62 represents the set of differential equations for the momentum and position or deformation of each element of the elastic adjusting spool where the number of element has been denoted by ‘n’. According to the Bond-graph

model of the elastic spool in Fig. 32, the number of q_dot62 equals to the number of element which is n. Therefore, the number of p_dot62 will be (n+1) as per the geometry of the elastic spool. It must be noted that the in the above code, $i = n$ and for the convenience of computation, both the state variables (momentum p, and deformation or location q) have been considered in a series of ith element instead of ith element for qi for and jth element for pj. While calculating q_dot62, equation (13) has been applied where $\dot{q}_\iota = q\_dot62$. Equations for the first ($q\_dot62(1)$) and last element ($q\_dot62(n)$) have been written separately as the inertia for the left and right ended element is half of the actual value. Similarly, calculation for p_dot62 has been done using equation (14) and as there are two mechanical forces acting on the 1st and last element of p_dot62, equations for $p\_dot62(1)$ and $p\_dot62(n)$ have been written in terms of those mechanical forces. Using Bond-graph model of control valve with elastic adjusting spool, equations for pdot62_fl and pdot62_fr have been derived following Bond-graph rules [26-31].

$$pdot62\_fl = b * ((1/I20 * p20 - b/I62 * p62\_fl) * (R34 + R29) + (1/I20 * p20 - b/I62 * p62\_fl - d/I39 * p39 - c/I62 * p62\_fl - f/I39 * p39) * R52 - Se53 + (1/I20 * p20 - b/I62 * p62\_fl - d/I39 * p39 - c/I62 * p62\_fl) * R48) + c * ((1/I20 * p20 - b/I62 * p62\_fl - d/I39 * p39 - c/I62 * p62\_fl - f/I39 * p39) * R52 - Se53 + (1/I20 * p20 - b/I62 * p62\_fl - d/I39 * p39 - c/I62 * p62\_fl) * R48); \quad (31)$$

$$pdot62\_fr = -1/C63 * q63; \quad (32)$$

Considering the above obtained set of equations for elastic adjusting spool, the equations for state variables of inlet pressure, feedback pipe pressure and control part pressure have been derived where Bond-graph rules for extracting mathematical model has been applied. Final formations of these equations are shown as follows:

$$pdot4 = Se1 + Se18 - (1/I4 * p4 + g/I39 * p39) * R2 - (1/I4 * p4) * R5 - (1/I4 * p4 - a/I39 * p39) * R12 - (1/I4 * p4 - a/I39 * p39 - 1/I20 * p20) * R19; \quad (33)$$

$$pdot20 = (1/I4 * p4 - a/I39 * p39 - 1/I20 * p20) * R19 - Se18 - (1/I20 * p20 - b/I62 * p62\_fl) * (R34 + R29) - (1/I20 * p20 - b/I62 * p62\_fl - d/I39 * p39 - c/I62 * p62\_fl - f/I39 * p39) * R52 + Se53 - (1/I20 * p20 - b/I62 * p62\_fl - d/I39 * p39 - c/I62 * p62\_fl) * R48 - (1/I20 * p20) * R24 - (1/I20 * p20) * R22; \quad (34)$$

$$pdot39 = a * ((1/I4 * p4 - a/I39 * p39) * R12 + (1/I4 * p4 - a/I39 * p39 - 1/I20 * p20) * R19 - Se18) + g * (Se1 - R2 * (1/I4 * p4 + g/I39 * p39)) + f * ((1/I20 * p20 - b/I62 * p62\_fl - d/I39 * p39 - c/I62 * p62\_fl - f/I39 * p39) * R52 - Se53) + d * ((1/I20 * p20 - b/I62 * p62\_fl - d/I39 * p39 - c/I62 * p62\_fl - f/I39 * p39) * R52 - Se53 + (1/I20 * p20 - b/I62 * p62\_fl - d/I39 * p39 - c/I62 * p62\_fl) * R48) - 1/C41 * q41 - (1/I39 * p39) * R42; \quad (35)$$

5.4 Simulation Results and Analysis:

To illustrate the elasticity or flexibility of the resultant elastic adjusting spool physically, a set of simulations has been performed including pure elastic vibration on the resultant adjusting spool. In this project, 5 uniform elements have been considered to form the discrete geometry of the elastic spool with the first and last element that receives external mechanical forces. It has been assumed that this discrete beam structure of the elastic spool is initially stress free in the room temperature and both side surfaces of the spool or beam structure is completely isolated. Thus, the obtained model can deliver pure elastic behaviour. A table for material parameters has been given below:

Table 2: Beam material parameters for elastic spool

No. of elements	n	5
Total mass	$M - total$	$0.3783\ kg$
Area of each element	A	$1.539e^{-4}$
Strain (aluminium)	E	$69e^{9}$
Total length	$L - total$	$0.1\ m$

In Fig. 35, the position of the 1st and last element of the elastic spool has been plotted together which demonstrates that the gap between the position of 1st element and last element is the summation of the total deformation of five elements. As all the elements of the discrete beam structure moves together as single elastic spool being lumped, changes in position of all elements can be represented by the change in position of 1st and last element. Moreover, the displacement of elastic spool's 1st and last element towards same direction causes an opening of adjusting orifice and the small zoom graph inside the figure represents the initial expansion and shrinking of 1st and last elements of elastic spool. This displacement of 1st and last element in opposite direction which occurs at the very beginning reveals the fact that the spool has enough elasticity with the dynamics of expansion and shrinking. The overall shrinking of this elastic spool (discrete beam structure) happens due to the mechanical forces acting on the both left and right end elements. Therefore, with the increase of adjusting orifice cross-section, more pressure flows in front zone of control spool and displacement of control spool causes a decrease in control orifice area. Thus, pressure in control part is regulated which proves that the control valve is working properly even with the elastic moving element.

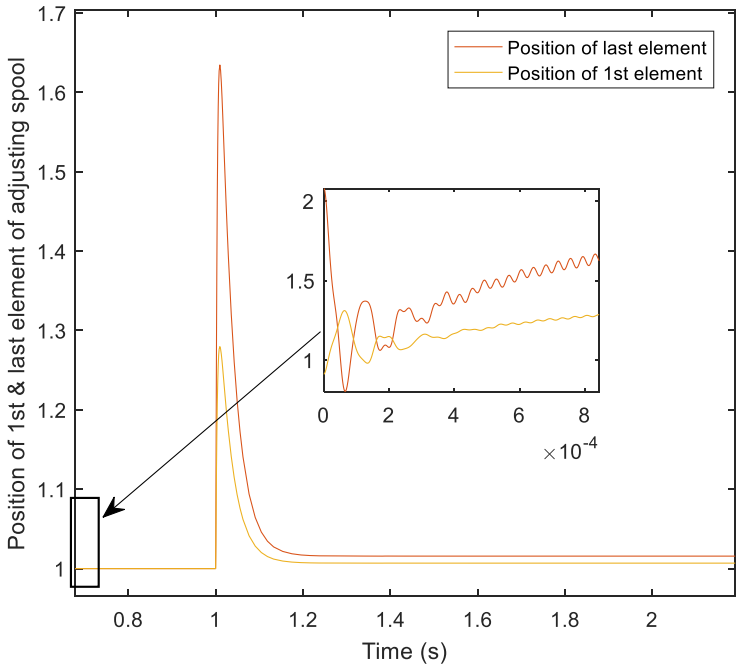

Figure 35: Position of 1st and last element of elastic adjusting spool.

From Fig. 36, the elasticity of the adjusting spool is more visible as it shows the initial amount of deformation of all 5 elements clearly. Following graph reveals the elasticity dynamic of the spool which denotes the structural shrinking of the discrete beam configuration. With the rigid spool, it is not possible to capture such dynamics of elasticity.

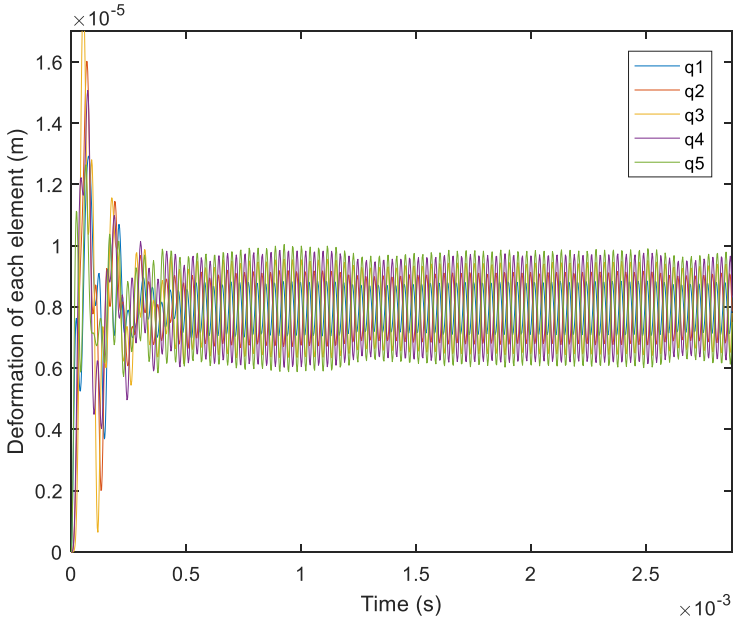

Figure 36: Deformation of each element of elastic adjusting spool at the beginning.

In Fig. 37, the same graph of Fig. 36 has been shown at time 1sec. The small zoom graph in the following figure clearly represents different amount of deformation of each element just after 1sec where according to the geometry of beam structure the amount of deformation of 1st element (q1) is more than the 2nd element (q2) and the amount of deformation of 2nd element is more than the 3rd element (q3) and so on. The summation of deformation of all 5 elements equals to the gap between the 1st and last element's position.

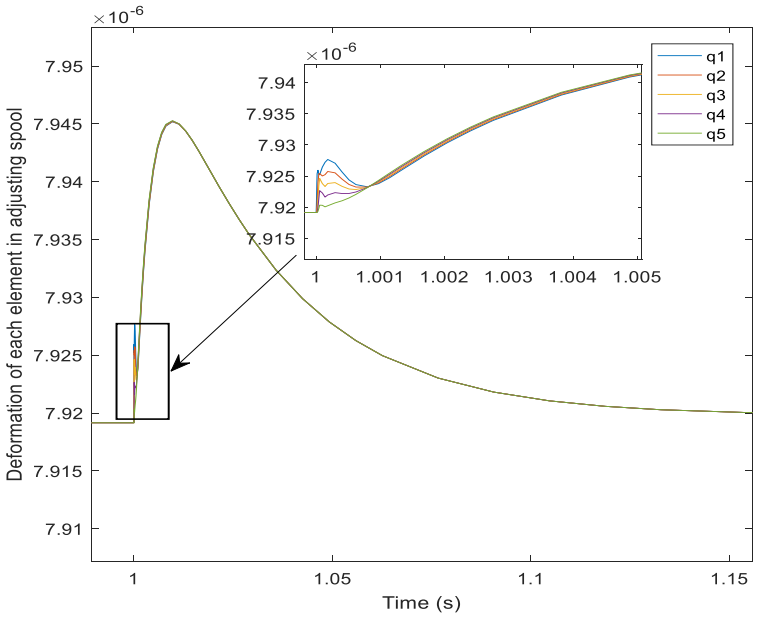

Figure 37: Deformation of each element of elastic adjusting spool.

Fig. 38 represents the corresponding changes in the momentum of each element caused by the deformation where a significant change in momentum is shown for the 1st and last element as both of them experience direct effect of mechanical forces.

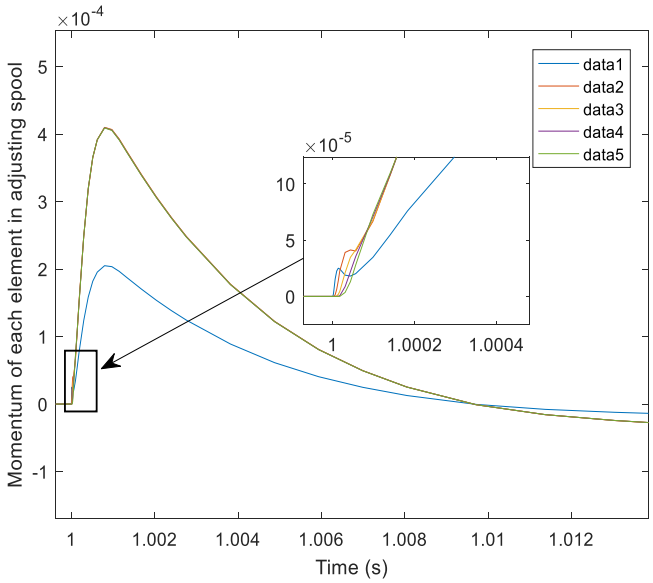

Figure 38: Momentum of each element of elastic adjusting spool.

The simulation results achieved from this chapter, demonstrate the capability of adjusting spool of being flexible enough to expose the dynamic of elasticity. The shrinking of elastic spool due to the external mechanical loadings coming from both left and right end elements proves the flexibility of adjusting spool explicitly.

6 Chapter 6: Addition of Thermal Impact to the System for Thermal Investigation

The obtained Bond-graph model of elastic spool in chapter 5 with its current configuration is not able yet to capture internal thermal impact. Therefore, in this chapter, thermo-mechanically enhanced elastic spool has been modelled by incorporating thermo-mechanical interactions into the existing purely elastic spool where the injected additions or alterations were consistent with Bond-graph technique. After the modelling of thermo-mechanically enhanced elastic spool, thermal impact has been added to the system and then simulation has been carried out to investigate the system's behaviour in presents of thermal conditions.

6.1 Modelling of Thermo-Mechanically Enhanced Elastic Spool:

In order to make the elastic spool capable of capturing structural expansion phenomena caused by unwanted thermal condition in the system, an equivalent source of effort has been added to the boundary junction of each element of the discrete beam structure[18]. This source of effort is capable of mimicking the impact of expansion dynamics and thus, can result a model of enhanced elastic spool on which the thermal investigation can be performed to reveal how the system dynamics are changed by the thermal condition. After inserting another energy port with thermal strain in each 1- junction of Fig. 32, the resultant expansive Bond-graph model of the spool is as shown in Fig. 39.

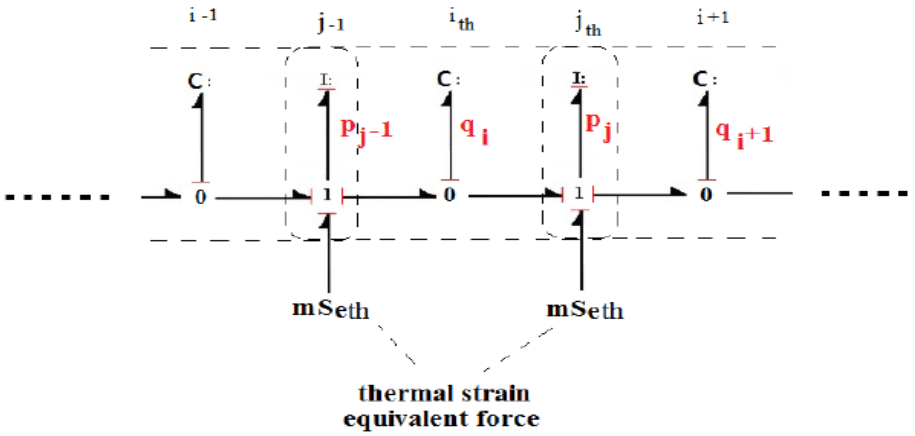

Figure 39: Bond-graph model of expansive beam structure.

According to this Bond-graph model of Fig. 39, the new governing equation of state variable of jth junction is driven from equation (14) which is:

$$\dot{p}_j = \frac{q_i}{C_i} - \frac{q_{i+1}}{C_{i+1}} + MSeth_j \qquad (36)$$

This additional thermal strain equivalent force, $MSeth_j$, may be expressed as[3, 18]:

$$MSeth_j = AE\alpha[(T_i - T_0) - (T_{i+1} - T_0)] \quad (37)$$

Where, A= the area of cross-section of each element
E= the elasticity modulus
α= the expansion coefficient
T_i= the temperature of ith element and
T_0= the reference temperature, room temperature.

Now, equations (25), (13), and (15) together establish the new set of state equations which govern the thermos-mechanically enhanced Bond-graph model of the elastic spool. Thus, with the addition of equivalent thermal effort source (26) into each element via jth junction, the rate of momentum for each element at its boundary has become a function of both the material parameters and temperature change of the adjacent elements. The resulting Bond-graph model therefore is now capable to address the dynamics of structural dilation via the kinematics of the discrete beam structure[20].

To determine the value of $MSeth_j$, the temperature change in each element has to be evaluated using the Bond-graph model of heat conduction as temperature is the effort in thermal domain. As per thermo-dynamics, entropy, $\dot{S}$ is the independent variable and temperature, T is the dependent variable. The product of theses variables is known as the thermal power which may be express as the rate of entropy, $\dot{Q}$:

$$\dot{S}T = \dot{Q}$$

By implementing this entropy flow, the resultant thermal model will be capable of receiving thermal power from various sub-domains as the resultant model will be domain neutral in nature.

According to the Bond-graph model of the heat conduction, proposed by Amir Zanj and Fangpo He [20], the state variable equation of each element in thermal sub-domain can be determined from the following Bond-graph model.

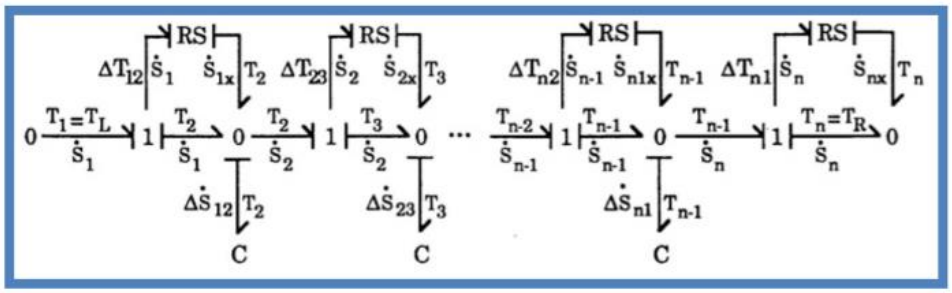

Figure 40: Bond-graph model of heat conduction [20].

In Fig. 39, an RS -component is a source of entropy used to generate entropy required for thermal domain. There is an additional entropy ($\dot{S}x$) caused by the temperature gradient which is added to the nearest 0 junction. Based on the causality of this bond-graph model of heat conduction, from the storage component C, the state variable of thermal extensive state, q_{thi}, for the ith capacitor can be derived. Considering the storage component C constant for each element, the effort or temperature of this storage element in terms of the state variable q_{thi}, can be calculated using following equation:

$$T_i = C(q_{thi}) = T_0 e^{\frac{1}{\rho v c}(q_{thi} - s_0)} \quad (38)$$

Where ρ, v and c are the density, volume and specific heat capacity of the element and s_0 denotes the entropy of ith element. Considering the Bond-graph presentation of Fig. 39, the equation of state variable of thermal extensive state is as followed:

$$\dot{q}_{thi} = \frac{1}{R_j}\left(C(q_{thi-1}) - C(q_{thi})\right) - \frac{1}{R_{j+1}}\left(C(q_{thi}) - C(q_{thi+1})\right) + S_i^{\dot{g}en} \quad (39)$$

Where R_j, is the resistance coefficient of the respective energy component which can be formulated as:

$$R_j = \frac{\Delta x T_j}{\lambda A} \quad (29)$$

Here λ and A are the specific thermal conductance coefficient and area of corresponding element. The length of each element is considered here to be equal of Δx which is the length from centre of one element to the centre of adjacent element. Fig. 40 clearly demonstrates the heat conduction process with a series configuration of three elements. Length of each element and both the R and C components are vividly observable from the following figure where storage component, C is at the centre of each element and resistance component, R is divided into both the boundaries of element. This heat

conduction schematic (RC – series) also illustrates that thermal energy is stored via one side of the element and dissipated from the other side.

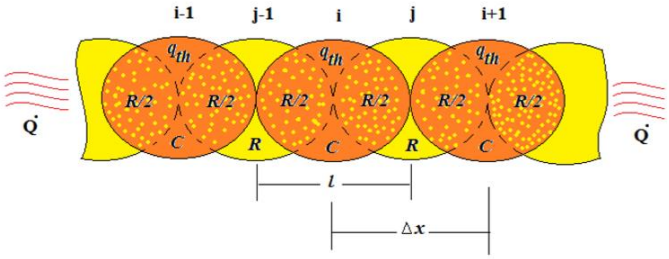

Figure 41: Schematic of 1D heat conduction [20].

T_j is the temperature at jth junction which is the difference between temperatures of two adjacent elements at their boundaries. The equation for T_j is as followed:

$$T_j = (T_{i-1} - T_i)/2 \tag{40}$$

Finally, to solve the equation of (28), the entropy generation rate, $S_i^{\dot{g}en}$, which is the irreversible entropy flow is calculated considering the Bond-graph model of Fig. 39. As per the power continuity theory of heat conduction [20]:

$$S_i^{\dot{g}en} = \frac{1}{R_j} T_0 e^{\frac{1}{\rho vc}(q_{thi} - s_0)} (e^{\frac{1}{\rho vc}(q_{thi} - s_0)} - 1)^2 \tag{41}$$

Now substituting this equation of $S_i^{\dot{g}en}$ for solving the equation (28), the desire state variable ($\dot{q}_{thi}$) equation of thermal-domain is achieved. With this state variable, equations (27) and (26) has been solved and thus the expression for mechanical strain has been obtained using the Bond-graph model of the heat conduction. At this stage, the obtained elastic spool with thermal strain is completely capable of capturing the structural dilation behaviour caused by the added thermal condition in the pressure control valve.

6.2 Simulation Results and Analysis:

A set of simulations was performed at this final stage, of the Bond-graph pressure control model with a thermos-mechanically enhanced elastic adjusting spool. The simulations involved heating and thermo-mechanical impact. The results obtained from these simulations not only illustrate the abilities of the adjusting spool but also reveals the dynamics of system in the presence of thermal load. The material parameters of the thermo-mechanically enhanced adjusting spool are provided in Table 3.

Table 3: Beam material parameters for Thermo-mechanically enhanced adjusting spool

Length	L	$2.1e^{-1}m$
Cross section area	A	$1e^{-4}m^2$
Mass	m	$5.67e^{-2}kg$
Conductivity	$\boldsymbol{\lambda}$	$2.73e^{2}\frac{J}{m.k}$
Density	ρ	$4e^{3}\frac{kg}{m^2}$
Reference entropy @298K	s_0	$2.83e^{1}\frac{J}{mol.k}$
Specific heat	c_p	$8.97e^{2}\frac{J}{kg.k}$
Volume	v	$4.2e^{-5}m^3$

To evaluate the efficacy of the Bond-graph model when addressing the thermal dynamics of structural dilation, a hot flow with a temperature of 450K was added to the system. Fig. 41 presents the temperature profile of each element of the adjusting spool. As the adjusting spool is isolated from both sides, according to the heat conduction schematic in Fig. 40, the temperature of the first element is greater than that of the second, and the temperature of the second element is greater than that of the third one, and so on. The simulation process was run for 200 seconds as the heat conduction from the first to last element required sufficient time to return viable results. From the figure, the temperature of the first element was raised to 385K from ambient room temperature, whereas the temperature of the last element was 299K.

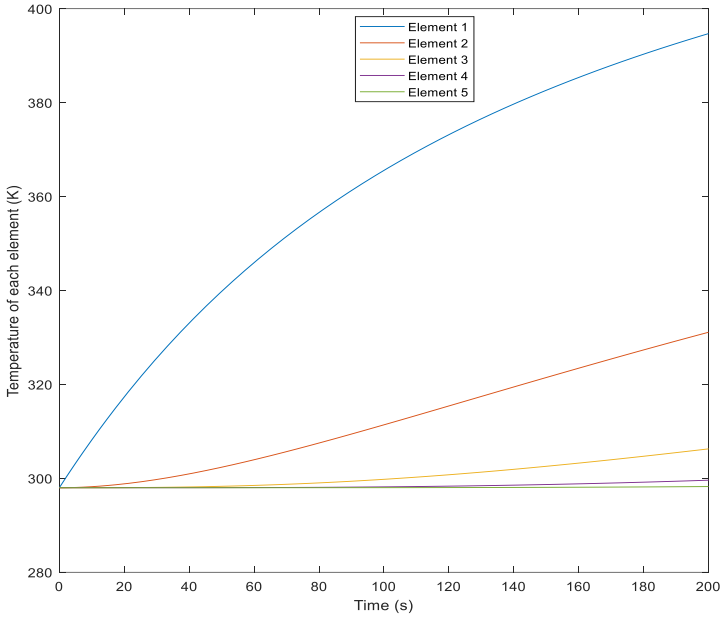

Figure 42: Temperature curve of each element of adjusting spool.

During the heat conduction process, as the temperature rise in each element was different, the deformation pattern of each element was different as shown in Fig. 42. The figure vividly illustrates that the deformation of the elastic spool is not homogeneous. There is an intense expansion experienced by the element (that is, the first element) nearest to the hot flow, whereas the expansions of other elements are comparatively lower.

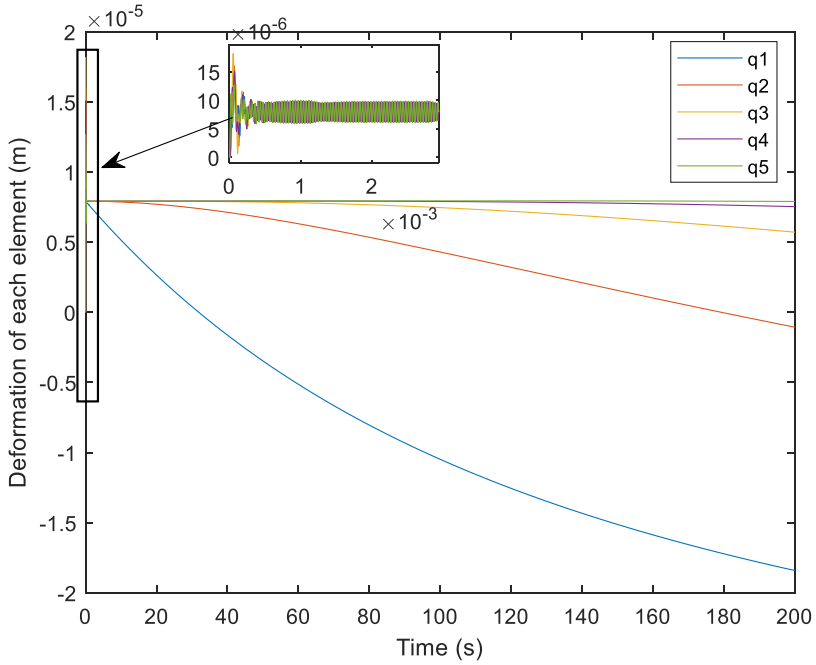

Figure 43: Deformation of each element of adjusting spool with thermal impact.

Due to the structural expansion of the spool, a significant displacement of first and last spool elements was observed, in opposite directions, as illustrated in Fig. 43. At the beginning of the heat conduction process, the displacement of the first and last elements is same as in Fig. 35. With the increase in temperature and deformation, the gap between the displacement of the first and last elements is increased. The displacement of the first element towards the closing of the adjusting orifice causes a pressure drop in the adjusting section, and thus, decreased pressure at the control spool front zone. A decrease in displacement of control spool therefore occurs, resulting in an opening of the control orifice as shown in Fig. 44.

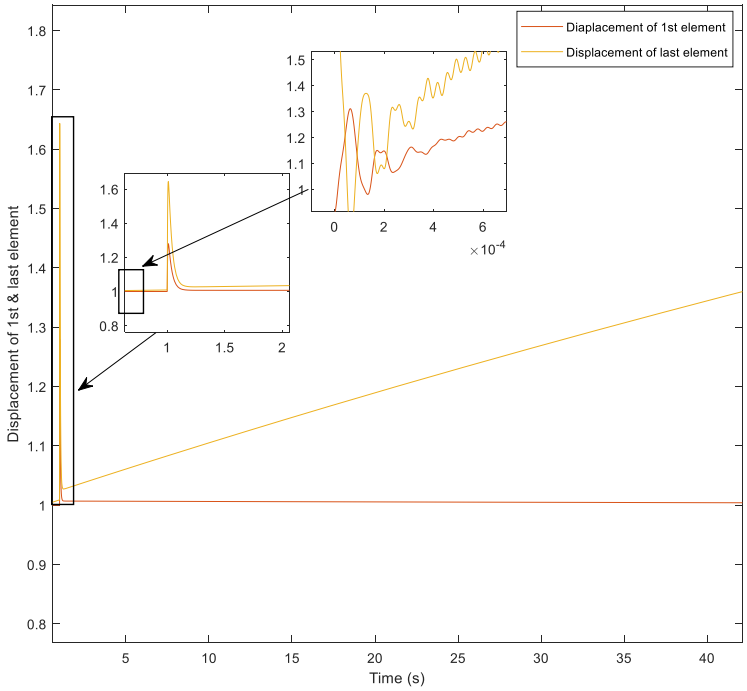

Figure 44: Displacement of 1st and last element of adjusting spool with thermal impact.

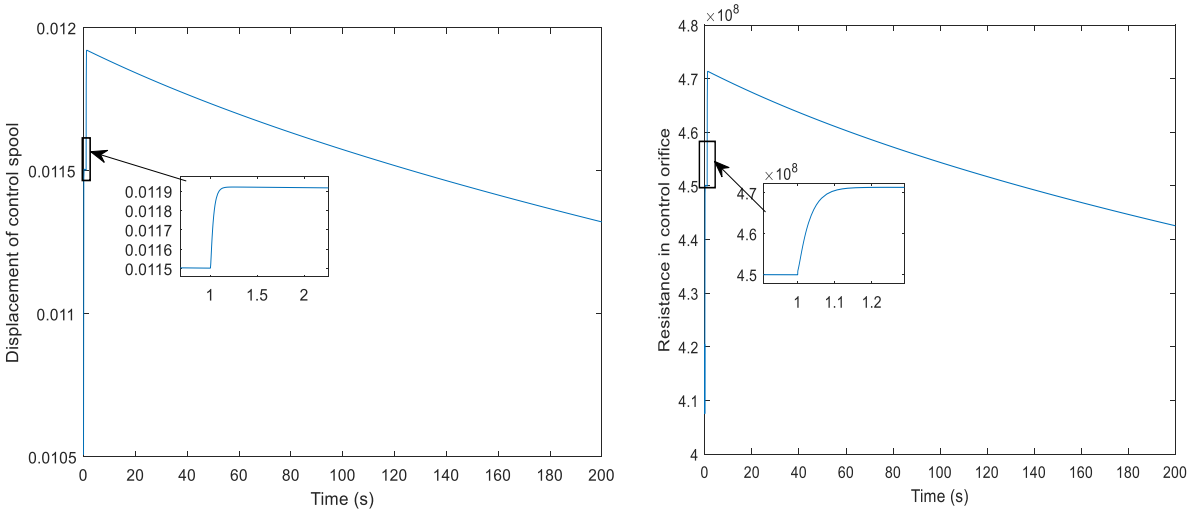

Figure 45: Displacement of control spool (left) and resistance of control orifice (right) with thermal impact.

From Fig. 44, the displacement of the control spool towards the opening of control orifice indicates that there is greater pressure from the inlet to the feedback pipe, and thus more pressure in the adjusting section. At this stage (if the valve was operating as intended) greater pressure on the adjusting spool will make it move toward an opening of adjusting orifice so that more pressure can flow through and push the control spool towards closing the control orifice. This is how the inlet pressure is supposed to

regulate. However, according to Fig. 45 there is a slow increase in pressure, meaning that the valve is no longer regulating pressure in presence of the thermal condition. Through the small zoom graph, it is shown that after 1 second, the valve regulates the pressure, and then as time increases, when the temperature of each element of the adjusting spool starts rising, the valve is not able to regulate the increase in pressure.

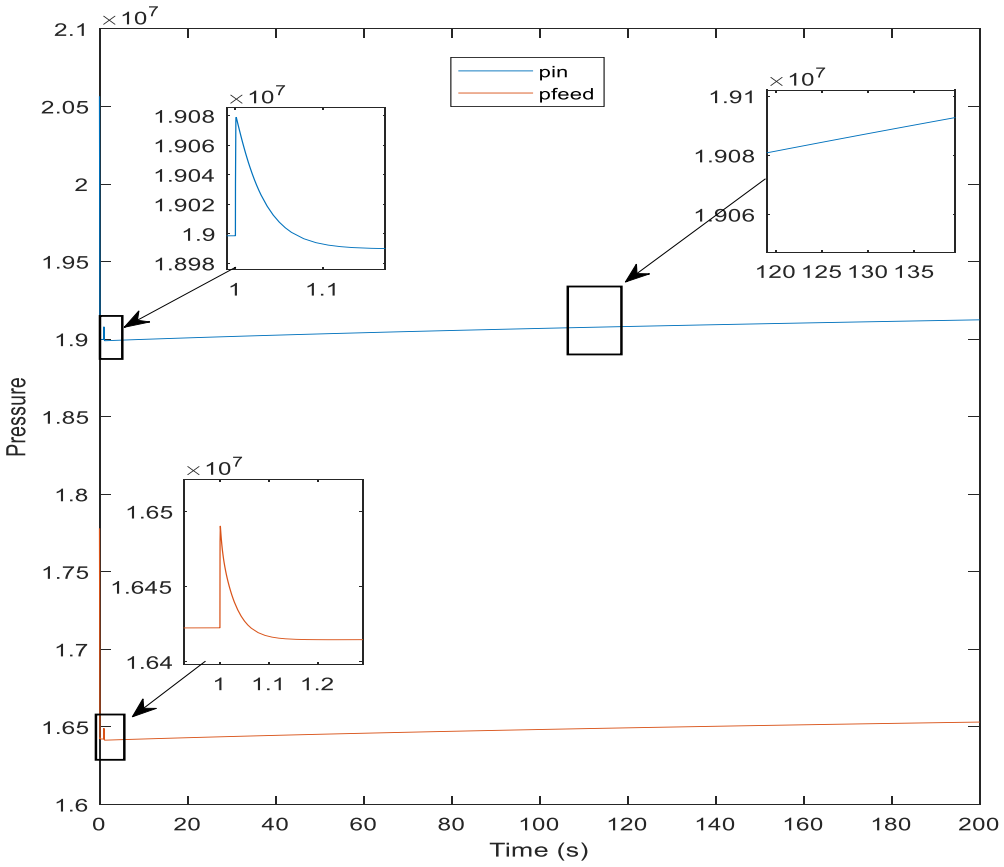

Figure 46: Valve's pressure regulation profile with thermal impact.

Through the simulation results obtained in this chapter, the capability of a thermo-mechanically enhanced spool in capturing system's dynamics in the presence of a thermal impact is illustrated precisely. It is clear that, with the slow dynamics of structural expansion, the operational set point of the control valve changes. Therefore, the level of operation also changes meaningfully due to the thermal impact. Such undesired behaviour of system can eventually prove catastrophic as it can make the entire system unstable.

7 Chapter 7: Conclusion

7.1 Project Conclusion:

This thesis investigates the thermal impact in a pressure control valve by means of the Bond-graph approach. To capture the thermal impact on such typical control valve, at first the existing pressure control valve is remodelled where modification is done in the adjusting section of the valve This modification involved eliminating the adjusting placoid or plate which is one of the moving elements in the control valve. The control valve initially had three moving elements as shown in Fig. 16, the control spool, the adjusting spool and the adjusting placoid. According to the valve's operational principle, the complexities regarding the modelling of the valve depend upon the simultaneous interaction of dynamics between the fluid flow and the moving mechanical elements. Modification of the adjusting section was performed to reduce such complexities. The resultant dynamics of the control valve with this modification revealed the accuracy of the modelling as well as the valve's efficacy in pressure regulation. The dynamics of the remodelled system in a wide range was established by comparing the simulation results from the remodelled system to the original.

Further modifications were made to the remodelled system to investigate the thermal phenomena in a control valve. At first, the two rigid moving elements (spools) were replaced with the elastic spools as the thermal phenomena cannot be captured with rigid spools. A Bond-graph model of the elastic spool was developed considering it as a discrete beam structure consisting of lumped elements. Thus, the obtained model of the spool had both the numerical and analytical characteristics which were required for delivering the dynamics of elasticity. The Bond-graph approach of modelling was best suited as the proposed model of elastic spool is required to reveal the dynamics of a multi-physical system (hydro-mechanical system). Simulation results at this stage confirmed the ability of the spool in delivering precise dynamics of elasticity.

Finally, a Bond-graph model of a thermo-mechanically enhanced spool was developed which was capable of addressing the thermal impact on the control valve. The resulting thermo-elastic spool delivered the dynamic of structural expansion caused by the thermal loading. To achieve this thermo-mechanically enhanced spool, the concept of equivalent thermal source was implemented. The thermal strain equivalent force was added to the Bond-graph model of the elastic spool via an extra energy port to each element. The thermal condition was then added to the system through the hot flow in the adjusting section. Final simulation results illustrated how the structural expansion occurred due to the temperature raise in each element of the spool and how this expansion changes the operational set point of the control valve where the valve is no longer capable of regulating the pressure. Thus, the dynamics of the system in the presence of thermal impact were successfully investigated by the thermo-mechanically enhanced adjusting spool.

This thesis explains the significance of unveiling the thermal phenomena explicitly which is an inevitable part of investigating the dynamics of control devices under thermal conditions. Additionally, the simulation results of the final stage not only establish the validity of the developed thermo-elastic model of the adjusting spool but also illustrate the possible benefits of the chosen approach (Bond-graph method) in revealing the true physical meanings or behaviours of the system during operation.

The primary application of such a control valve is a space vehicle hydraulic control system in which lack of attention to such an unwanted thermo-mechanical condition may result not only in an irretrievable state of the control valve but also of a failure in the space propulsion system.

7.2 Recommendations:

There are two recommendations for the further development of this investigation on thermal impact which include:

I. Replacement of rigid control spool with the thermo-mechanically enhanced one:

In this thesis, investigation on thermal impact has performed only with adjusting spool where the thermo-mechanically enhanced model of the spool has been developed with the help of Bond-graph method. There is another moving element, the control spool of the valve, which is also required to be replaced with a thermo-mechanically enhanced one. To develop a Bond-graph model of thermo-mechanically enhanced control spool, same procedures are needed to be followed that have been performed for developing the adjusting one. Firstly, a Bond-graph model of elastic control spool is required to be developed considering the discrete beam structure geometry. Then, a new Bond-graph model of the control valve (remodelled one) is needed to be developed with the elastic control spool which has already been done. Fig. 46 represents the Bond-graph model of the control valve with both elastic control spool and adjusting spool. At this stage, the thermal strain equivalent source should be added via an extra energy port to develop the elastic spool as a thermo-mechanically enhanced one. Thus, following the same steps as taken for modelling thermo-mechanically enhanced adjusting spool, the thermo-mechanically enhanced control spool can be developed by means of Bond-graph method.

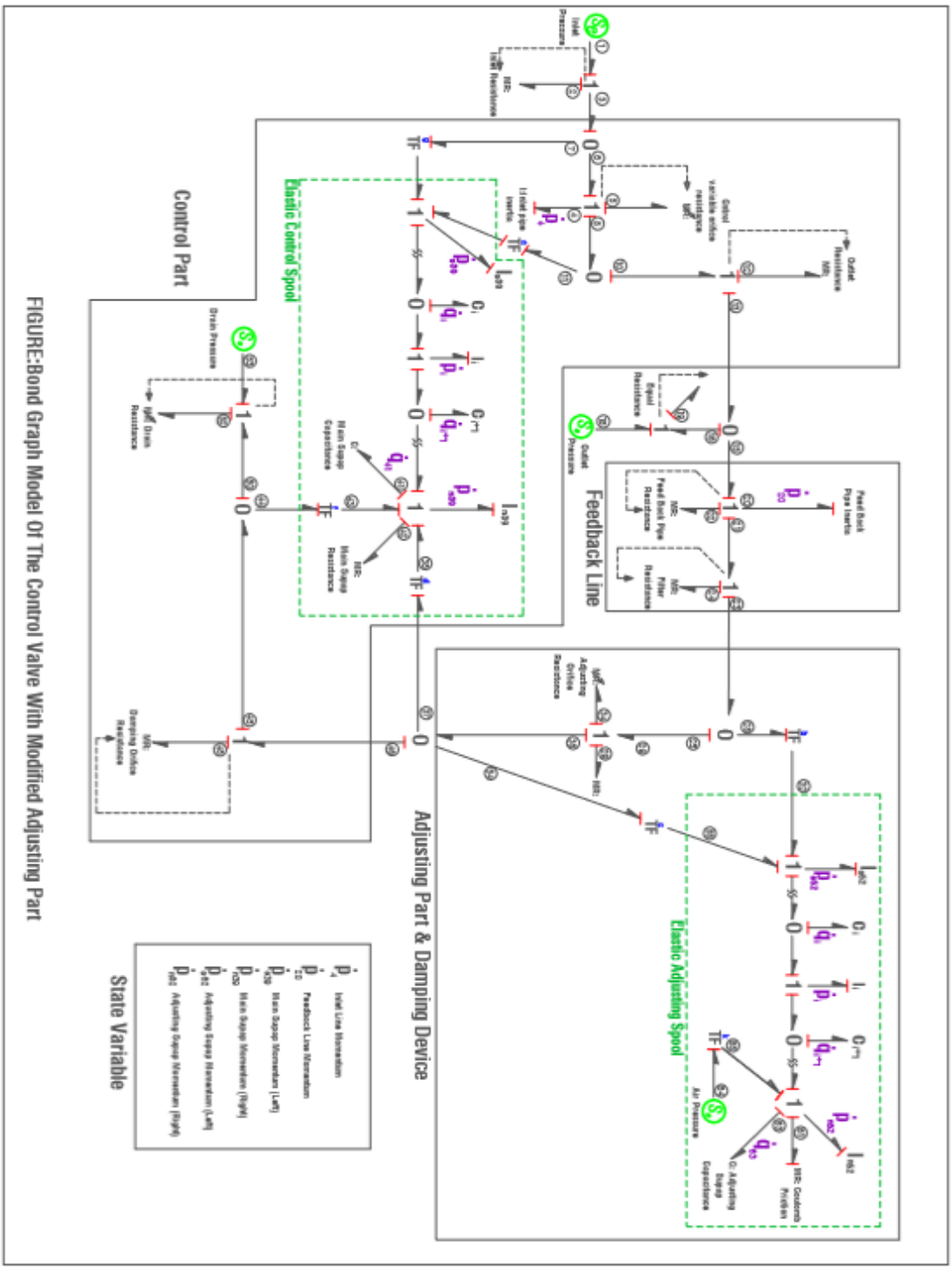

Figure 47: Bond-graph model of the Control valve with elastic control and adjusting spools

II. Addition of material softening dynamic in elastic spool Bond-graph model:

Material softening can be defined as the weakening of the system's stiffness while heating a struture under mechanical loading. In order to add this dynamic into the existing thermo-mechanically enhanced spool, the capaticance component, C in Fig. 39 needs to be replaced with a modulated C which is MC. The resultant Bond-graph model of thermo-mechanically enhanced sool with modulated MC is given below:

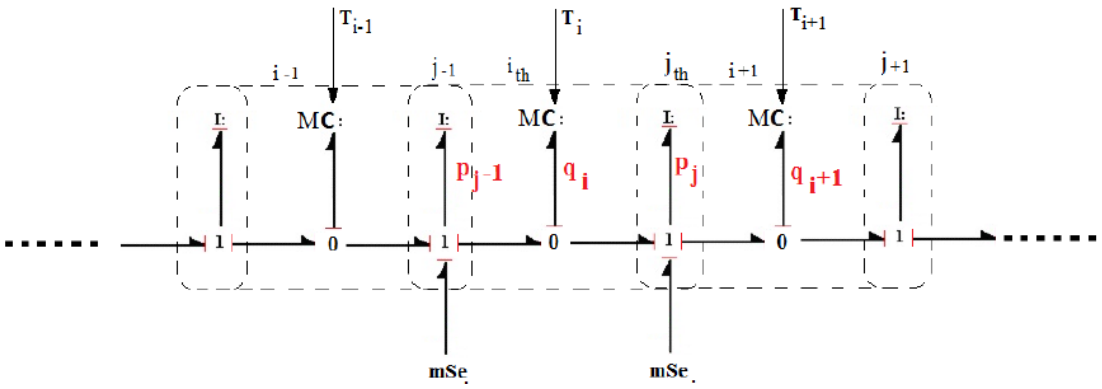

Figure 48: Bond-graph model of thermo-mechanically enhanced spool with material softening dynamic [18]

The coefficient for modulated storage element of MC for the elastic spool can be derived from following equation [18]:

$$MC = \frac{Lr_0^{n+1}(1+\alpha_L(T_i-T_0)^{n+1}}{(m-n)n\alpha} \quad (42)$$

Where m and are the constants for an arbitrary material and α_L and r_0 are the linear thermal expansion coefficient and function of unstressed atomic separation at room temperature respectively.

8 Appendix: MATLAB Code

The MATLAB codes for each simulation (from Chapter 4 to 6) are reserved within the Advance Control Research Group, Flinders University. The MATLAB codes can be provided upon request.

9 References

[1] A. Zanj, H. Karimi, A. Gholi, and M. Shafiee, "Dynamic modeling of indirect hydro-control valve–Bondgraph approach," *Simulation Modelling Practice and Theory,* vol. 28, pp. 65-80, 2012.

[2] H. Karimi, A. Nassirharand, and A. Zanj, "Integration of modeling and simulation of warm pressurization and feed systems of liquid propulsion systems," *Acta Astronautica,* vol. 69, no. 5-6, pp. 258-265, 2011.

[3] A. Zanj, F. He, and P. C. Breedveld, "Domain-Independent Thermoviscoelastic Modeling Framework: A Physical Approach on Thermoelasticity by Bond Graph," *Journal of Thermophysics and Heat Transfer,* vol. 32, no. 1, pp. 61-79, 2017.

[4] J. L. Baliño, "Finite Element Formulation for Computational Fluid Dynamics Framed Within the Bond Graph Theory," in *Bond Graphs for Modelling, Control and Fault Diagnosis of Engineering Systems*: Springer, 2017, pp. 311-358.

[5] J. Oden and D. Kross, "Analysis of general coupled thermoelasticity problems by the finite element method," in *Proceedings of the Second Conference on Matrix Methods in Structural Mechanics (AFFDL-TR-68-150)*, 1968, pp. 1091-1120.

[6] A. Ray, "Dynamic modeling and simulation of a relief valve," *Simulation,* vol. 31, no. 5, pp. 167-172, 1978.

[7] J. Watton, *Fundamentals of fluid power control*. Cambridge University Press, 2009.

[8] Y. C. Shin, "Static and dynamic characteristics of a two stage pilot relief valve," *Journal of dynamic systems, measurement, and control,* vol. 113, no. 2, pp. 280-288, 1991.

[9] A. Mukherjee and R. Karmakar, *Modelling and simulation of engineering systems through bondgraphs*. Alpha Science Int'l Ltd., 2000.

[10] W. Borutzky, "A dynamic bond graph model of the fluid mechanical interaction in spool valve control orifices," *Bond Graphs for Engineers,* pp. 229-236, 1992.

[11] W. Borutzky, G. Dauphin-Tanguy, and J. Thoma, "Advances in bond graph modelling: theory, software, applications," *Mathematics and computers in simulation,* vol. 39, no. 5-6, pp. 465-475, 1995.

[12] D. Karnopp, D. Margolis, and R. Rosenberg, "System dynamics: modeling and simulation of mechatronic systems, 2000," ed: John Wiley & Sons, NY, 1997.

[13] V. Dolga and L. Dolga, "Modelling and simulation of mechatronic systems," *Mecatronica,* no. 1, 2004.

[14] P. C. Breedveld, "Thermodynamic bond graphs: a new synthesis," *International Journal of Modelling and Simulation,* vol. 1, no. 1, pp. 57-61, 1981.

[15] A. Zanj and F. He, "Multi-Physical System Variable DoF Modeling."

[16] A. Zanj and H. H. Afshari, "Dynamic analysis of a complex pneumatic valve using pseudobond graph modeling technique," *Journal of Dynamic Systems, Measurement, and Control,* vol. 135, no. 3, p. 034502, 2013.

[17] H. H. Afshari, A. Zanj, and A. B. Novinzadeh, "Dynamic analysis of a nonlinear pressure regulator using bondgraph simulation technique," *Simulation Modelling Practice and Theory,* vol. 18, no. 2, pp. 240-252, 2010.

[18] A. Zanj, F. He, and P. C. Breedveld, "An energy-based viscoelastic model for multi-physical systems: A Bond graph approach," in *Systems, Man, and Cybernetics (SMC), 2016 IEEE International Conference on*, 2016, pp. 002214-002219: IEEE.

[19] S.-J. Zhu, X.-T. Weng, and G. Chen, "Modelling of the stiffness of elastic body," *Journal of sound and vibration,* vol. 262, no. 1, pp. 1-9, 2003.

[20] A. Zanj and F. He, "Conduction Model Compatible for Multi-Physical Domain Dynamic Investigations: Bond Graph Approach," *International Journal of Mechanical, Aerospace, Industrial, Mechatronic and Manufacturing Engineering,* vol. 10, no. 3, pp. 524-535, 2016.
[21] J. U. Thoma, *Simulation by bondgraphs: introduction to a graphical method*. Springer Science & Business Media, 2012.
[22] P. J. Gawthrop and G. P. Bevan, "Bond-graph modeling," *IEEE control systems,* vol. 27, no. 2, pp. 24-45, 2007.
[23] W. Borutzky, "Bond graph based physical systems modelling," *Bond Graph Methodology: Development and Analysis of Multidisciplinary Dynamic System Models,* pp. 17-88, 2010.
[24] J. F. Broenink, "Introduction to physical systems modelling with bond graphs," *SiE Whitebook on Simulation Methodologies,* vol. 31, 1999.
[25] W. Borutzky, "Bond graph modelling and simulation of multidisciplinary systems–An introduction," *Simulation Modelling Practice and Theory,* vol. 17, no. 1, pp. 3-21, 2009.
[26] K. Edge and D. Johnston, "The impedance characteristics of fluid power components: relief valves and accumulators," *Proceedings of the Institution of Mechanical Engineers, Part I: Journal of Systems and Control Engineering,* vol. 205, no. 1, pp. 11-22, 1991.
[27] A. Zanj, A. Kalabkhani, M. Abdous, and H. Karimi, "Modelling, simulation, and optimization of a hot pressurization system for a liquid propellant space engine and comparison with experimental results," *Proceedings of the Institution of Mechanical Engineers, Part G: Journal of Aerospace Engineering,* vol. 224, no. 10, pp. 1141-1150, 2010.
[28] H. Merritt and H. E. Merritt, *Hydraulic control systems*. John Wiley & Sons, 1967.
[29] O. A. B. Valero, *Preliminary Performance Study of Sherwood Regulator*. ProQuest, 2006.
[30] D. McCloy and H. R. Martin, "Control of fluid power: analysis and design," *Chichester, Sussex, England, Ellis Horwood, Ltd.; New York, Halsted Press, 1980. 505 p.,* 1980.
[31] D. Karnopp, D. L. Margolis, and R. C. Rosenberg, *System Dynamics: A Unified Approach, 2nd*. New York: Wiley. xiv, 1990.